

Full Waveform inversion

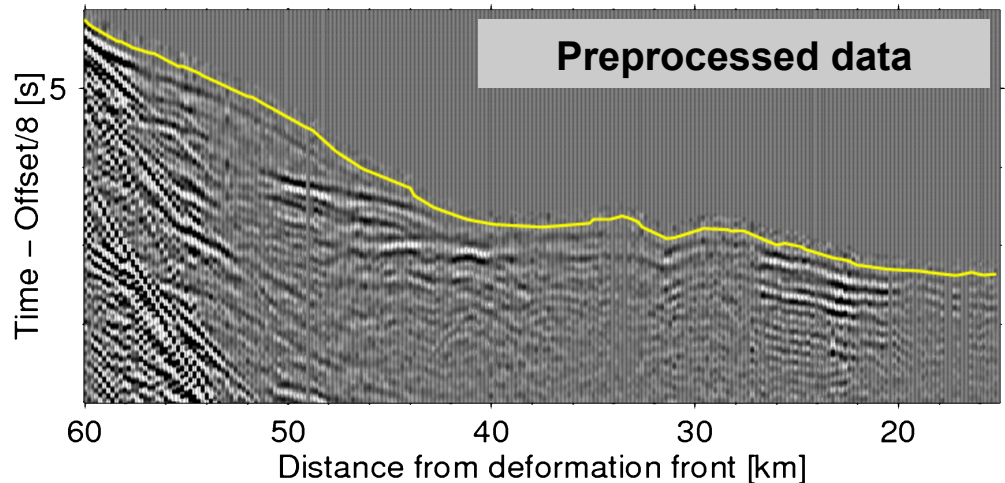
*Beyond ray theory,
Towards full waveform*

*Rie Kamei
Western University*

Acknowledgement

- Heiner Igel, Greta Kueppers, Celine Hadzioannou
- Andreas Fichtner
- Phillip Knaute, Andrea Colombi, Lubica Valentova, Andrew Valentine, Alan Schiemenz
- R. Gerhard Pratt, Andrew Brenders, Michael Afanasiev, Brendan Smithyman
- Takeshi Tsuji
- Vincent Etienne

Power of Waveform Inversion: Active seismic experiments from Nankai subduction zone

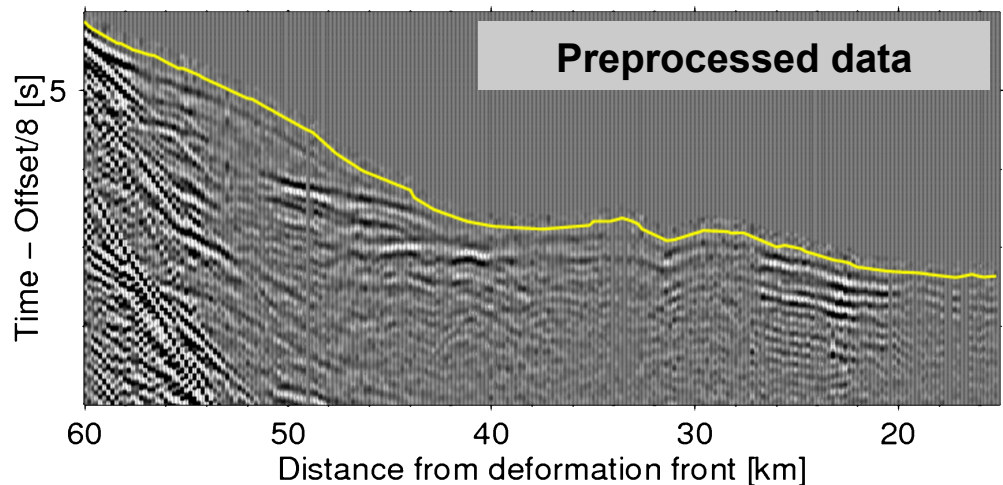
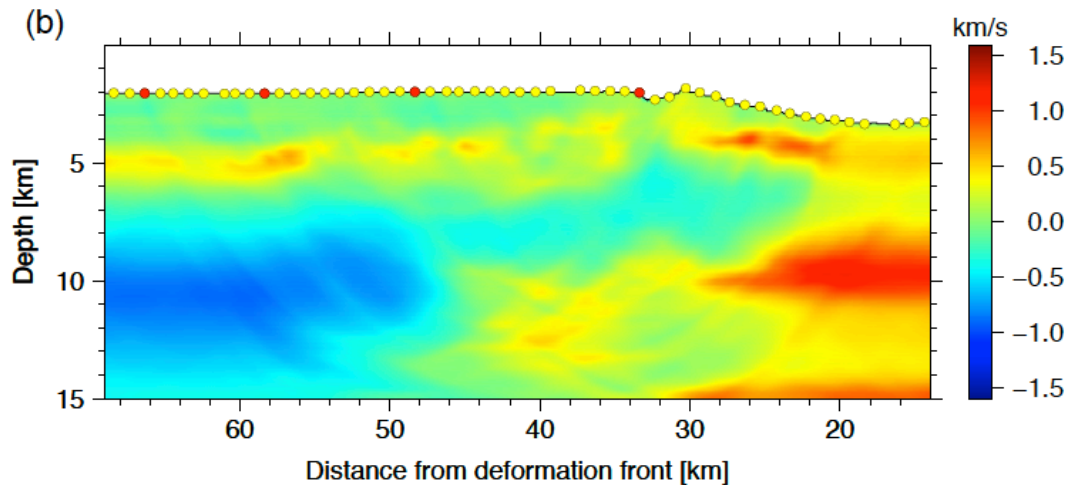


Kamei, R., Pratt, R. G., Tsuji, T. et al.. (2012). EPSL

Power of Waveform Inversion: Active seismic experiments from Nankai subduction zone

Travelttime Tomography

(b)



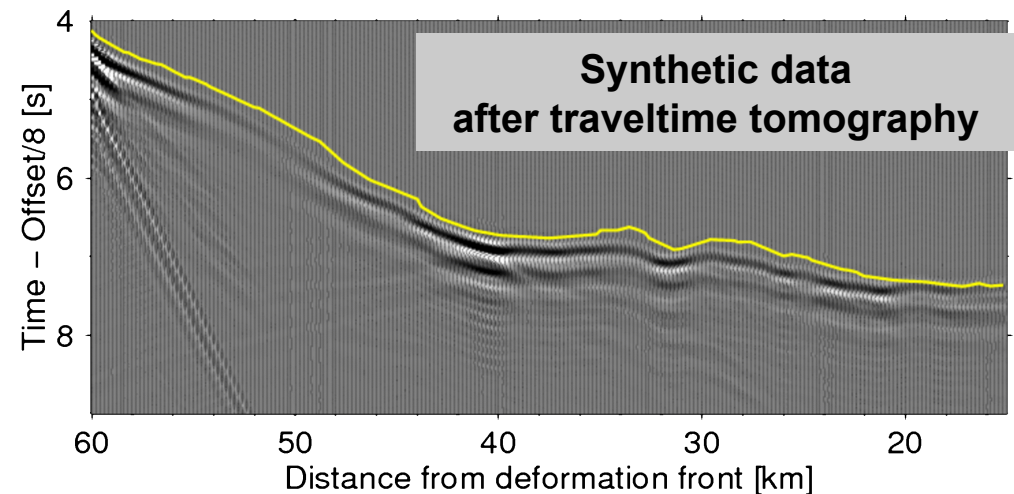
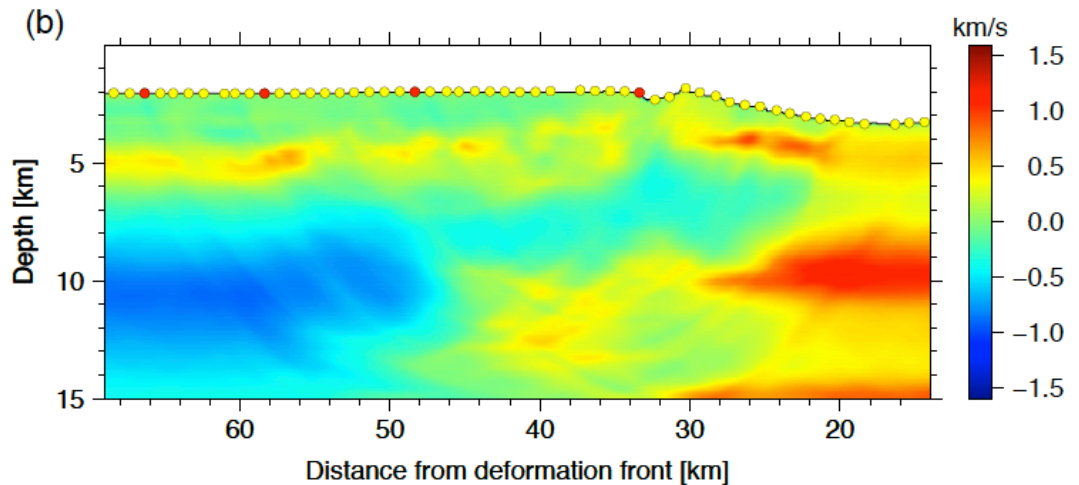
Kamei, R., Pratt, R. G., Tsuji, T. et al.. (2012). EPSL

Nakanishi, A., Kodaira, S., Miura, S., Ito, A., Sato, T., Park, J.-O., Kido, Y., et al. (2008). JGR

Power of Waveform Inversion: Active seismic experiments from Nankai subduction zone

Travelttime Tomography

(b)

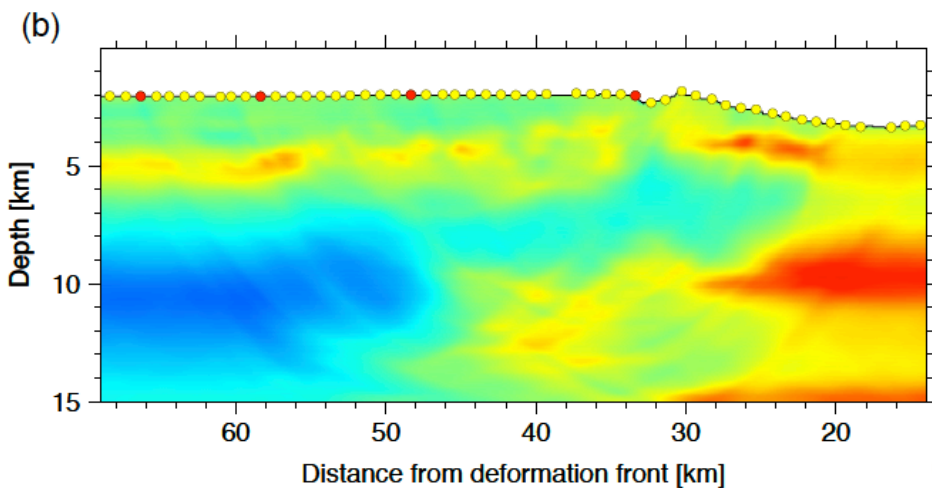


km/s
1.5 Kamei, R., Pratt, R. G., Tsuji, T. et al.. (2012). EPSL

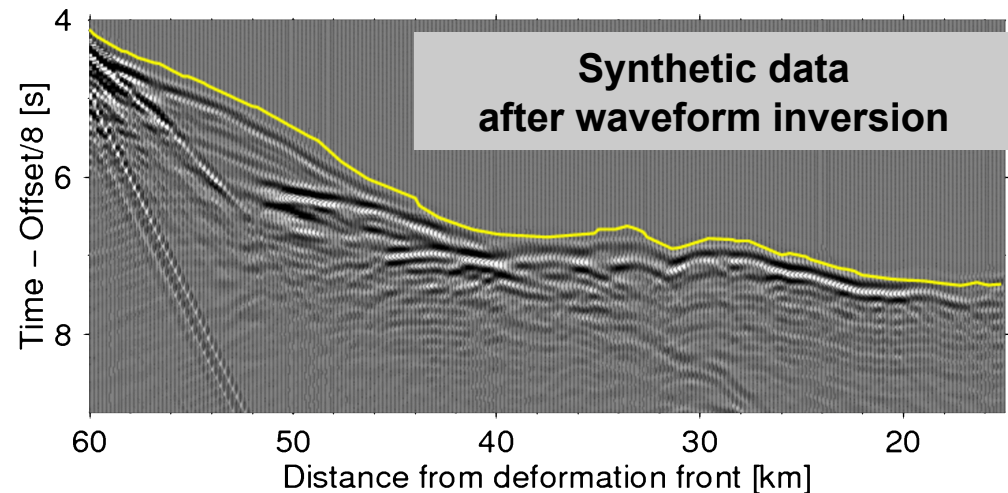
Nakanishi, A., Kodaira, S., Miura, S., Ito, A., Sato, T.,
Park, J.-O., Kido, Y., et al. (2008). JGR

Power of Waveform Inversion: Active seismic experiments from Nankai subduction zone

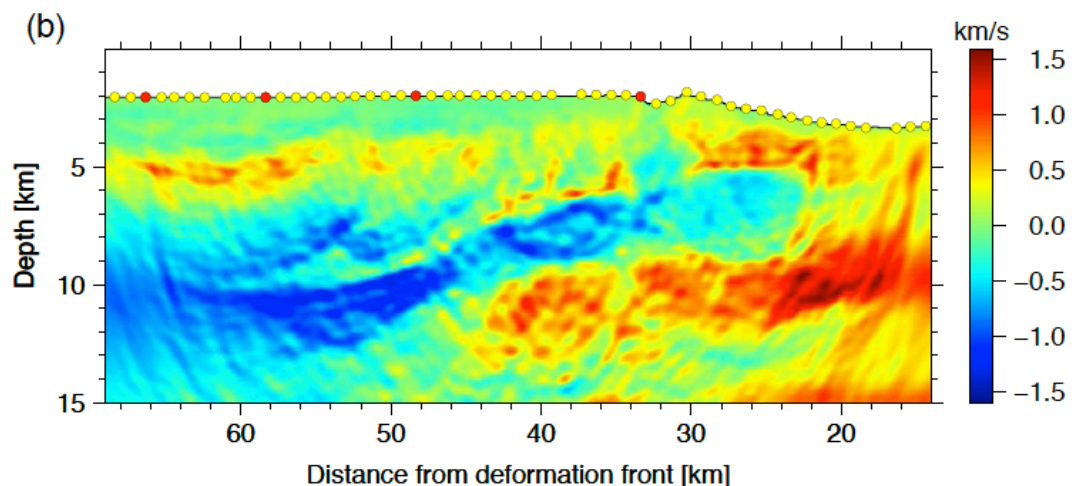
Travelttime Tomography



Nakanishi, A., Kodaira, S., Miura, S., Ito, A., Sato, T., Park, J.-O., Kido, Y., et al. (2008). *JGR*



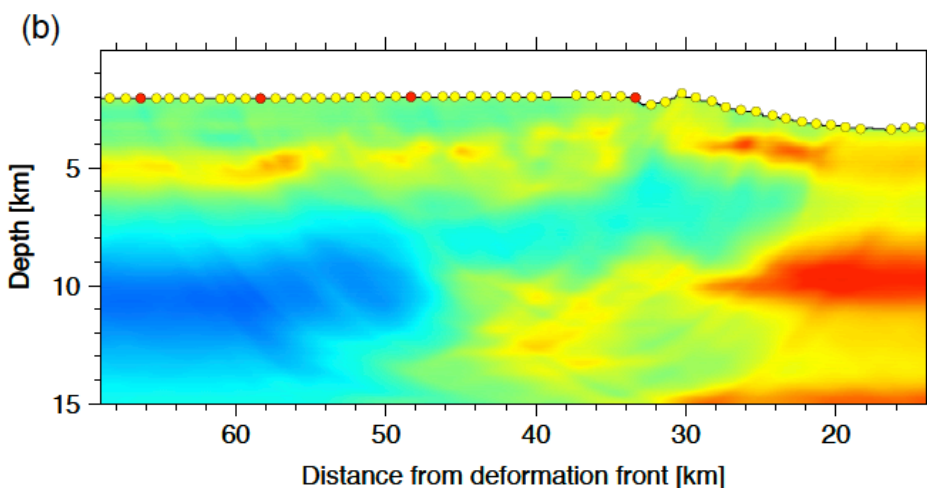
Waveform Inversion



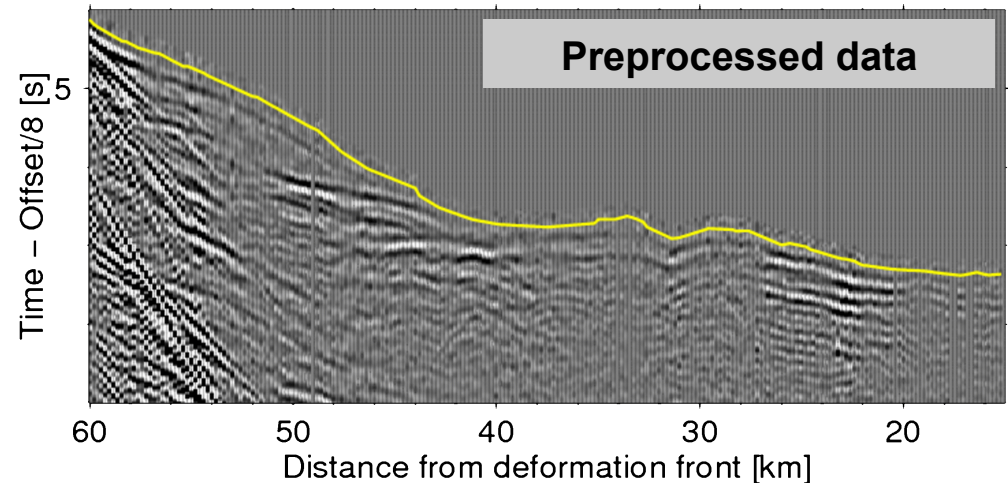
Kamei, R., Pratt, R. G., Tsuji, T., et al.. (2012). *EPSL*

Power of Waveform Inversion: Active seismic experiments from Nankai subduction zone

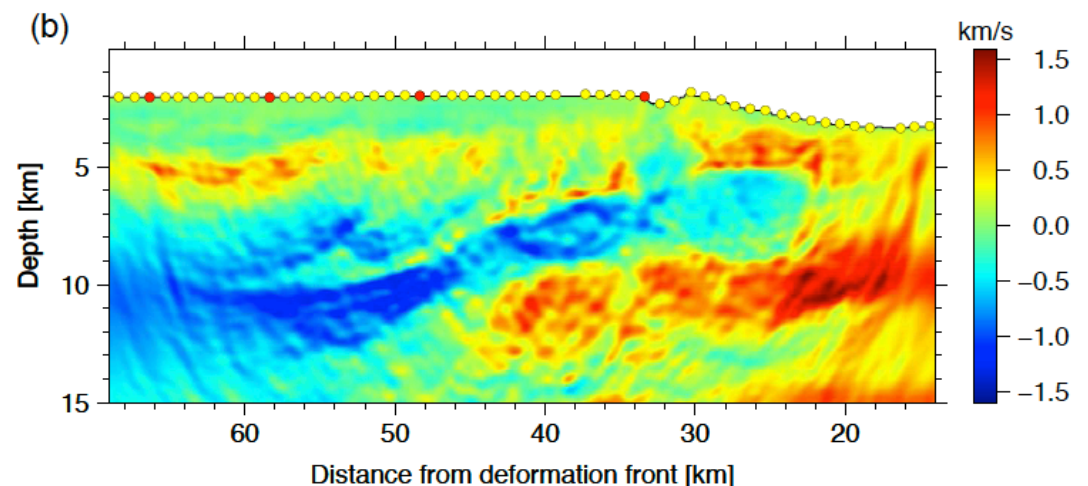
Travelttime Tomography



Nakanishi, A., Kodaira, S., Miura, S., Ito, A., Sato, T., Park, J.-O., Kido, Y., et al. (2008). *JGR*



Waveform Inversion



Kamei, R., Pratt, R. G., Tsuji, T. et al.. (2012). *EPSL*

Outline

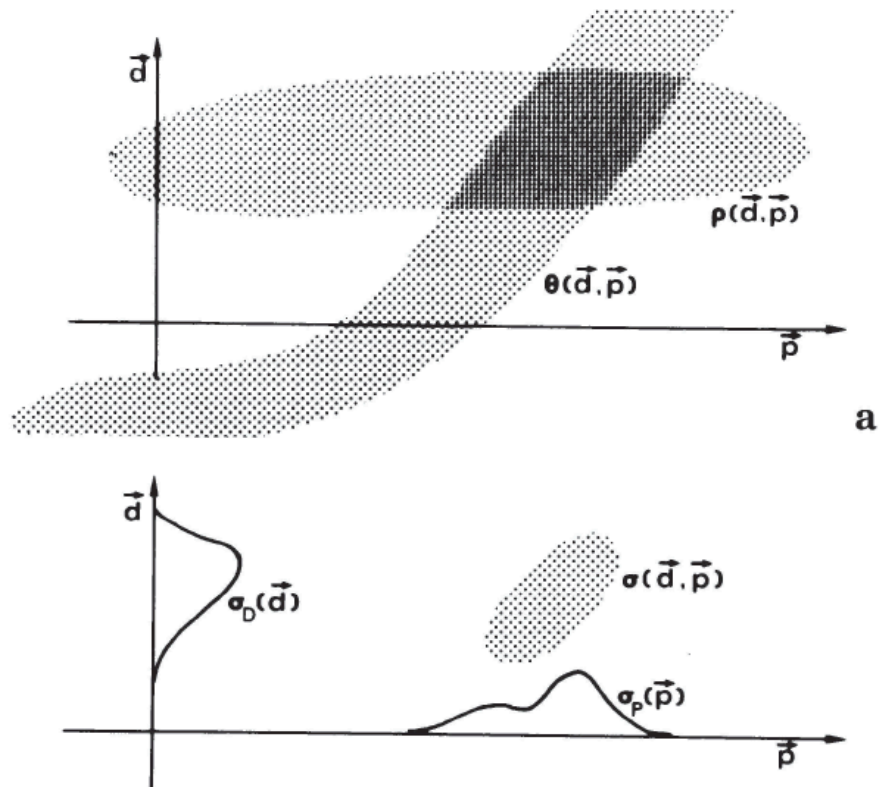
- Waveform inversion
 - Problem statement
 - Workflow
- Examples: A tour through scales

Goal of full waveform inversion

Using **full waveforms = P + S + surface waves**
and **accurate waveform modeling code**,
describe **probability distribution** of elastic parameters
(ideally full 21 parameters)

which accounts for

- waveform misfit
- modelization errors
- measurement errors
- priori knowledge about model



Tarantola, A., & Valette, B. (1982). J. Geophys.

Practical goal of (full) waveform inversion

Using **most significant component of waveforms** and **feasible numerical waveform modelling code**, obtain **one model + uncertainty** of most robust, non-unique parameters by **non-linear local optimization**:

$$\min \text{ waveform misfit} + \text{regularization term}$$

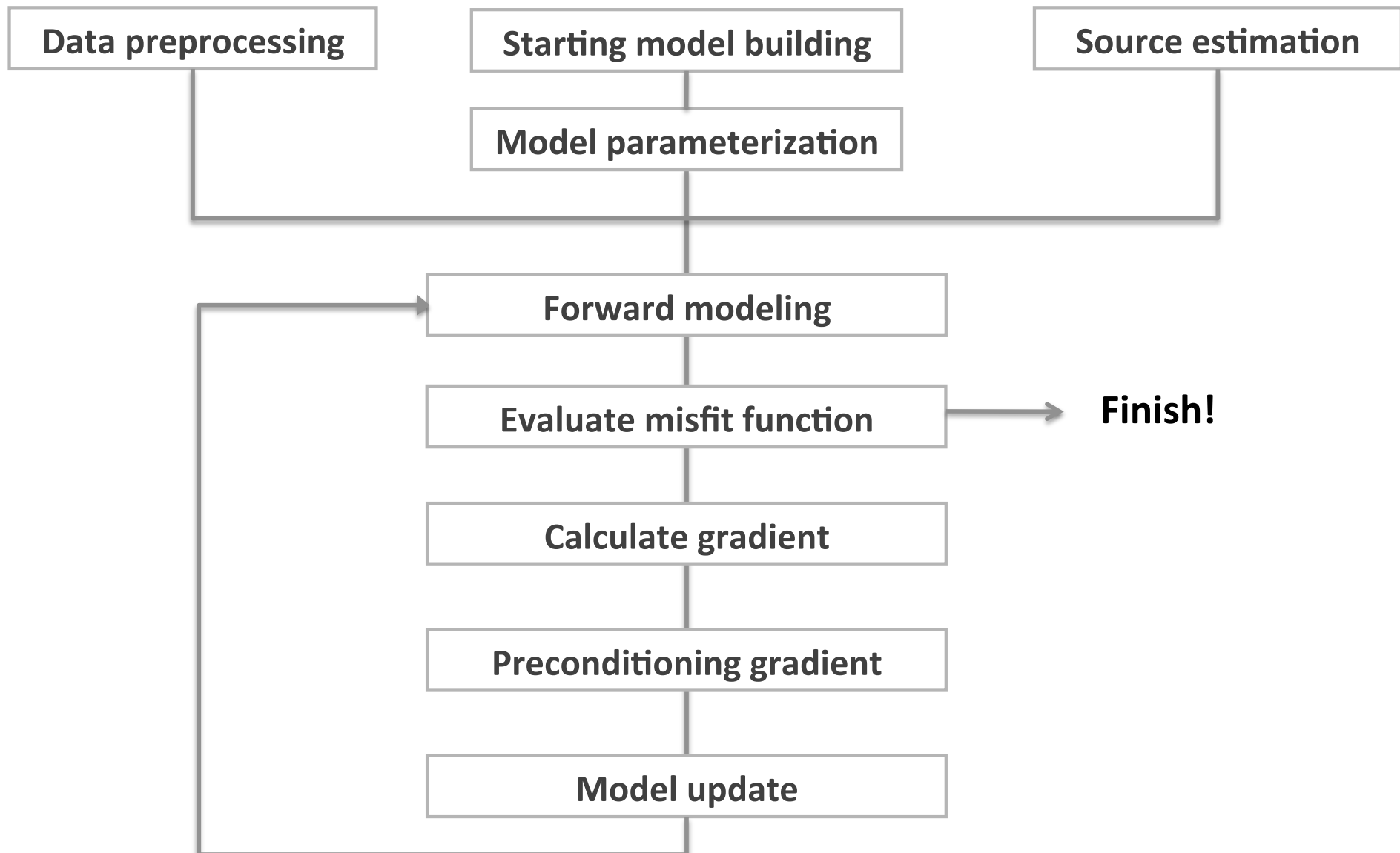
which incorporate

- measurement errors
- priori model knowledge

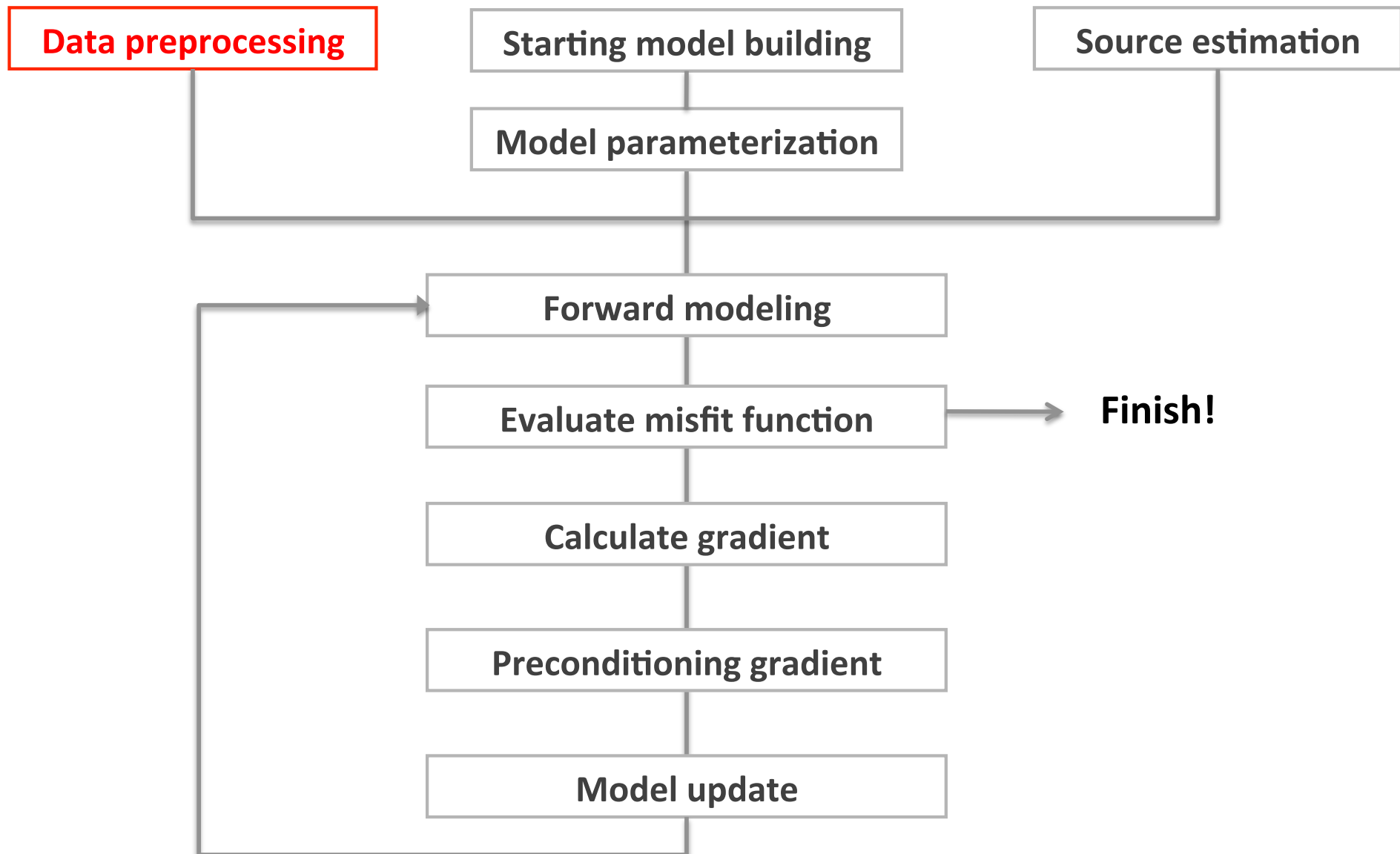
Outline

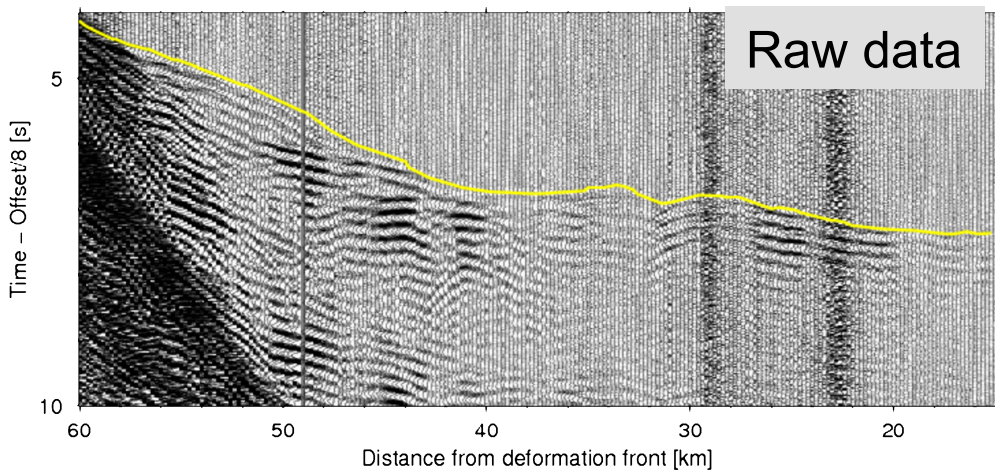
- Waveform inversion
 - Problem statement
 - Workflow
- Examples: A tour through scales

Workflow

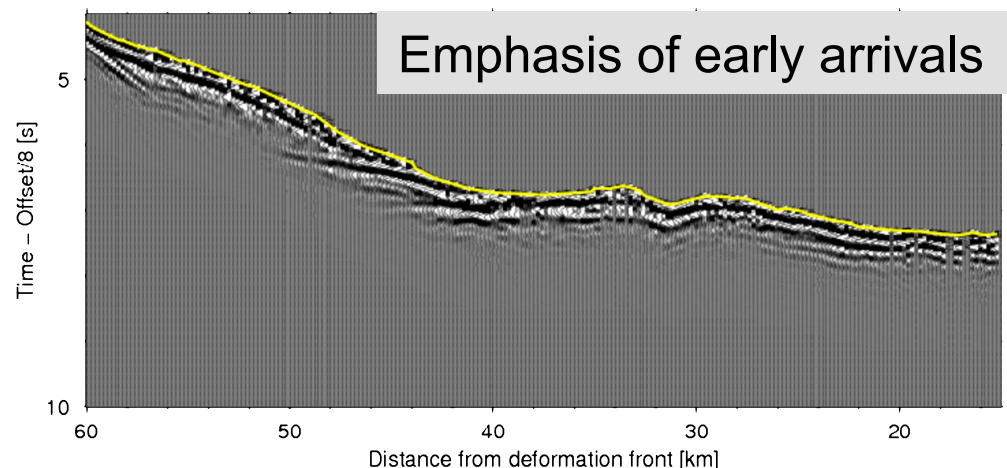
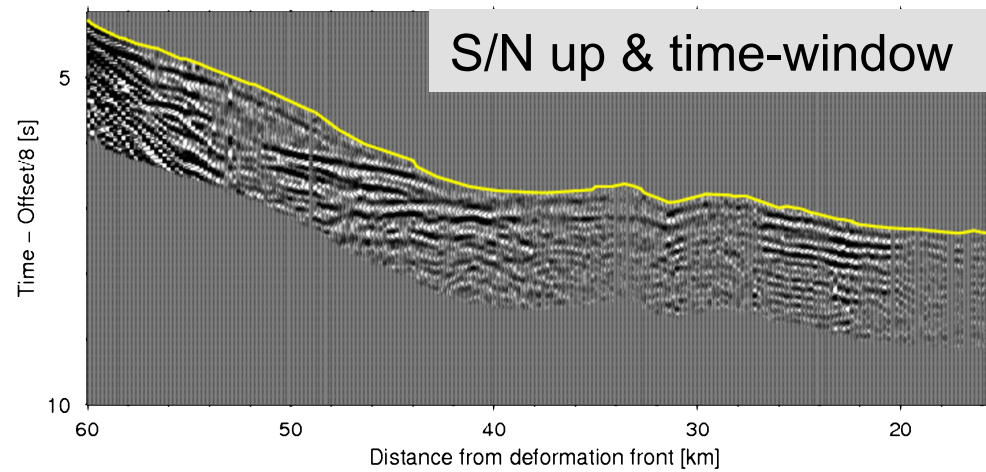


Workflow

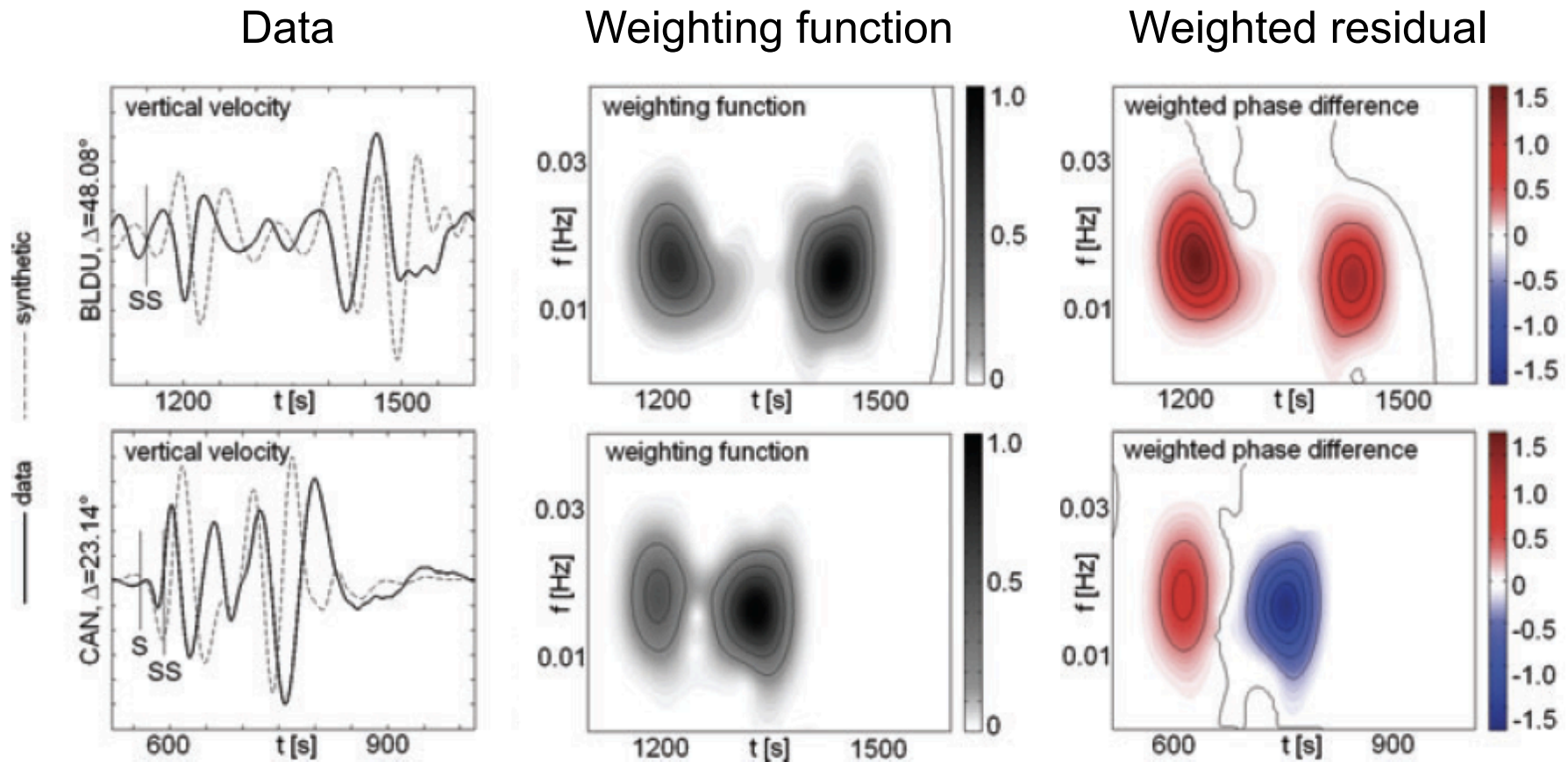




Preprocessing

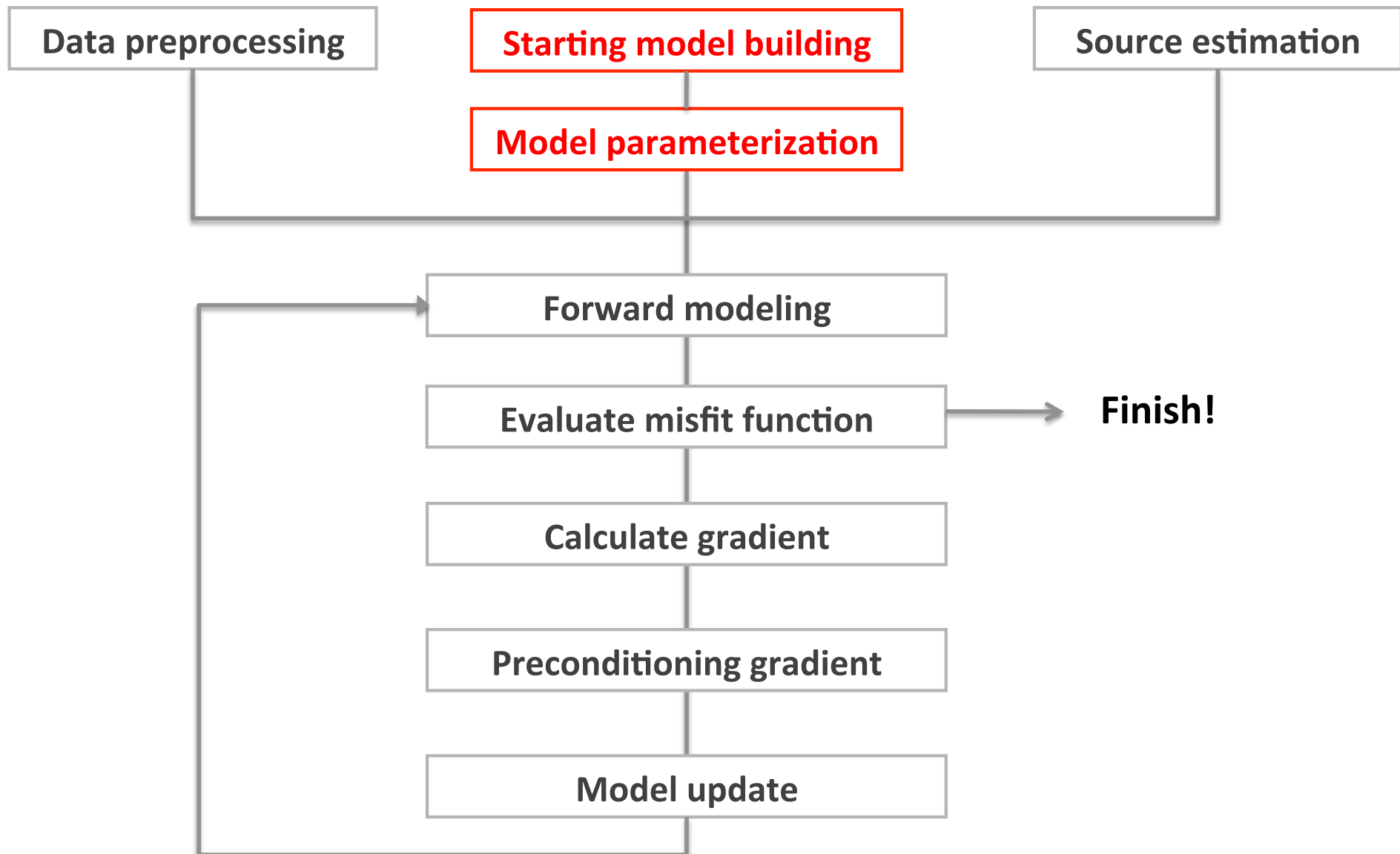


Preprocessing

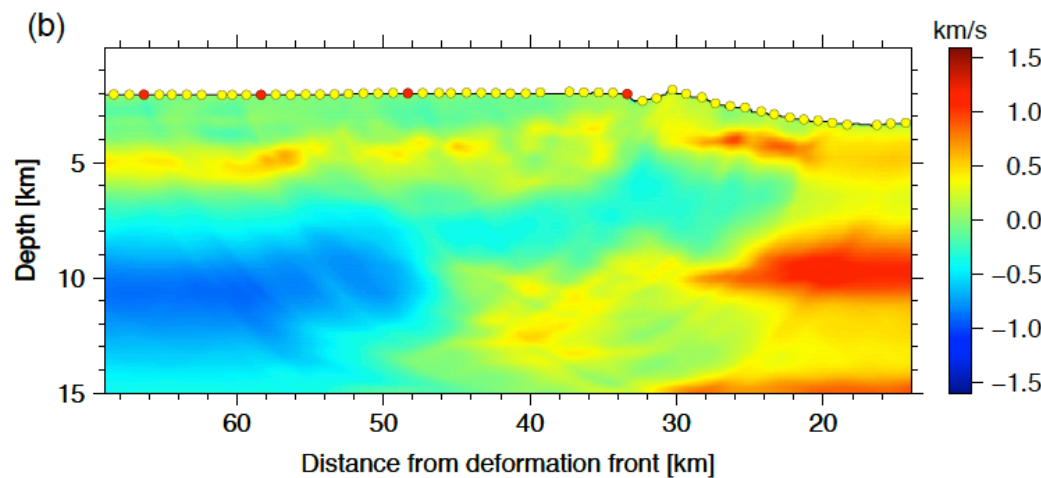


Modified from Fichtner, A., Kennett, B. L. N., Igel, H., & Bunge, H.-P. (2009). GJI

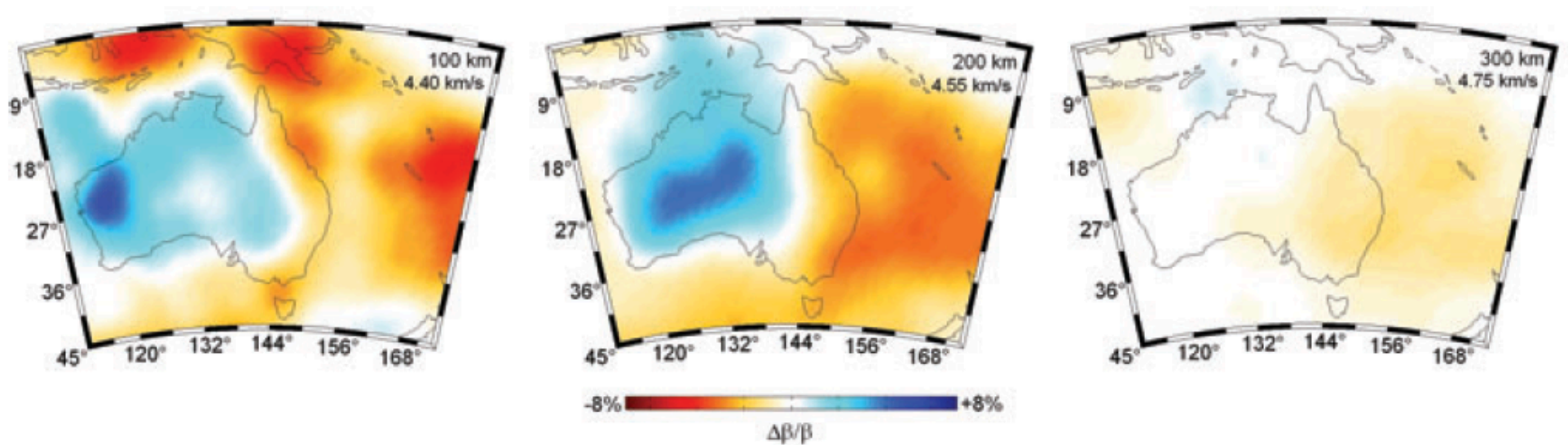
Workflow



Starting model

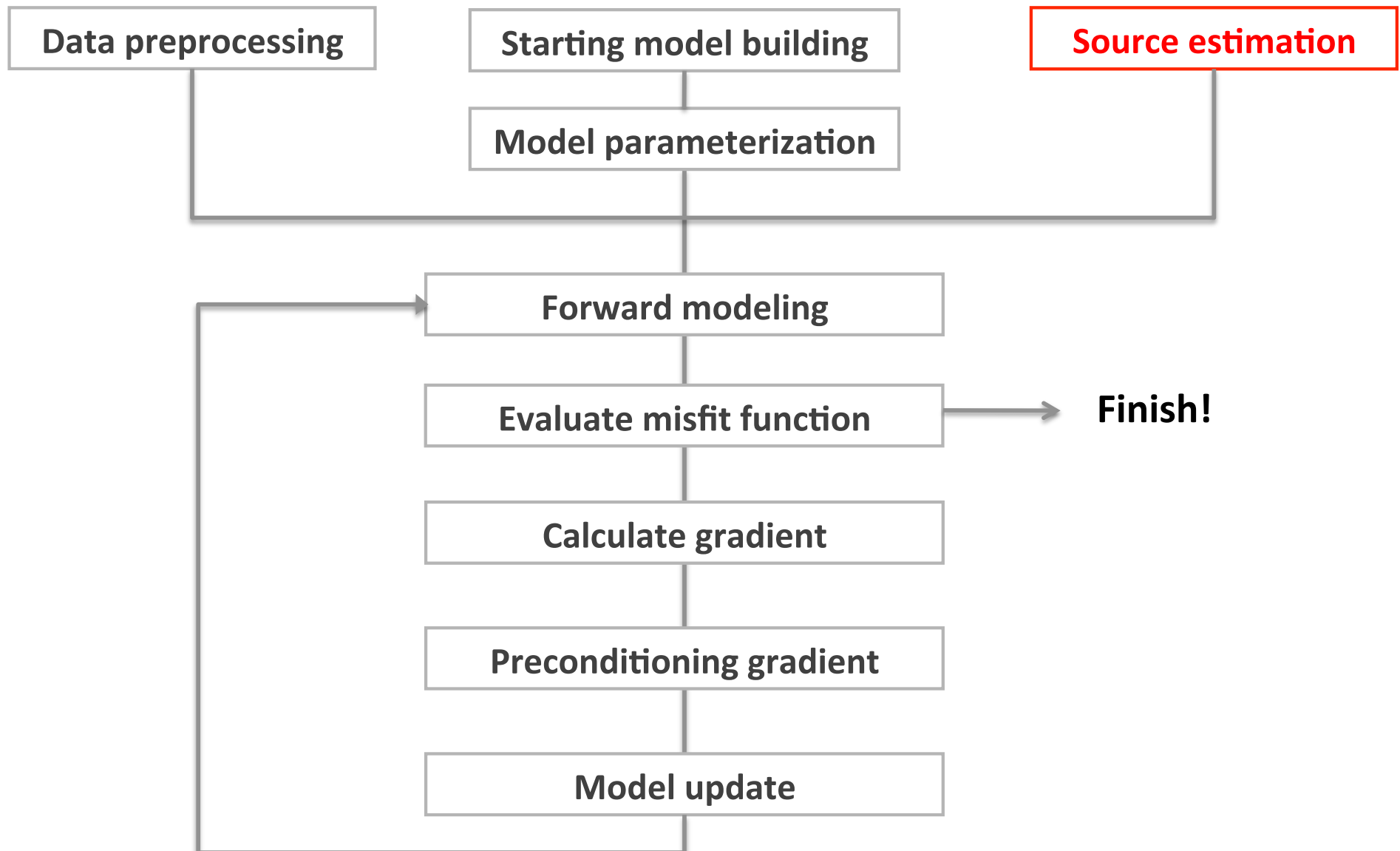


Kamei, R., Pratt, R. G., Tsuji, T., (2012), EPSL

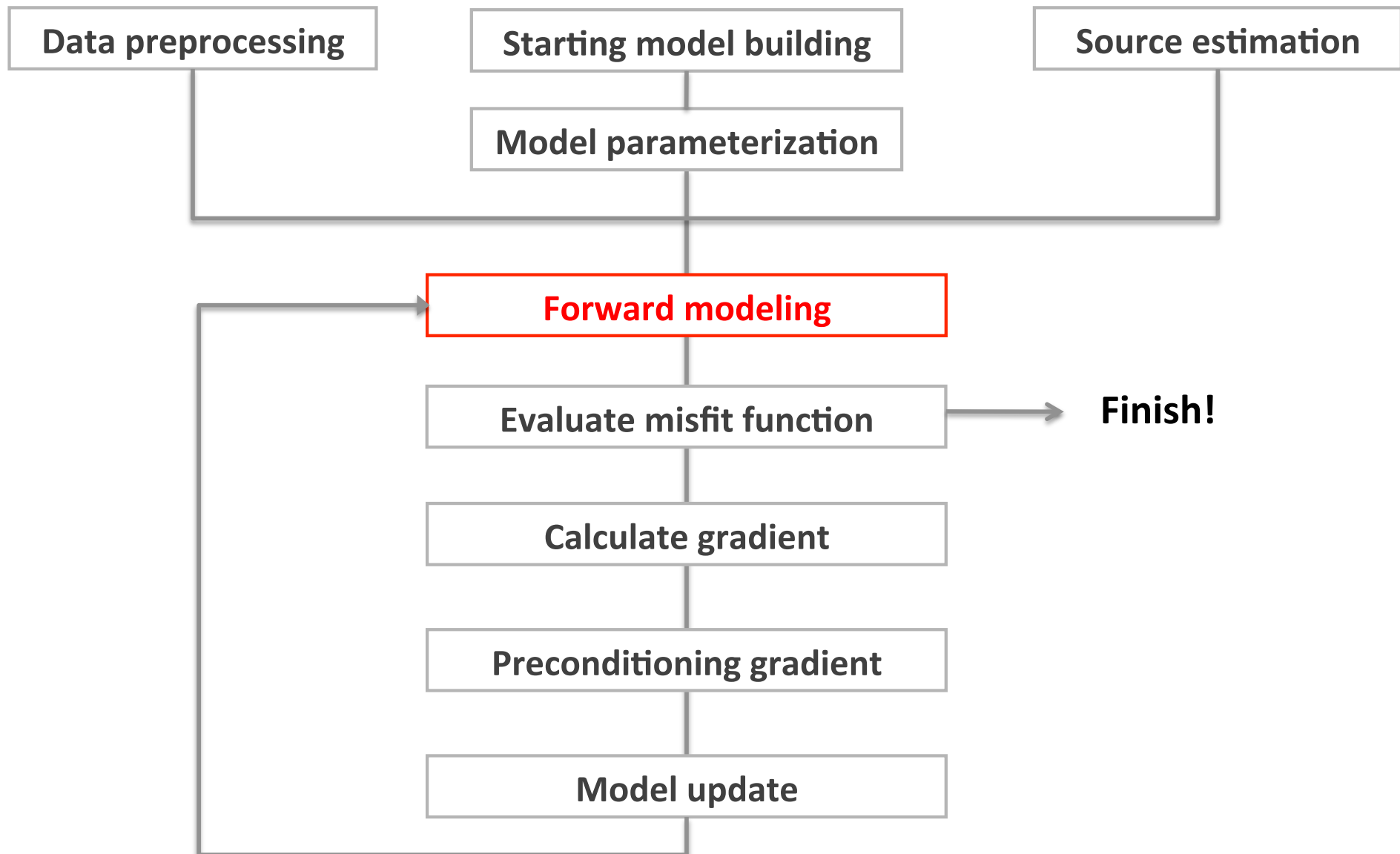


Fichtner, A., Kennett, B. L. N., Igel, H., & Bunge, H.-P. (2009). GJI

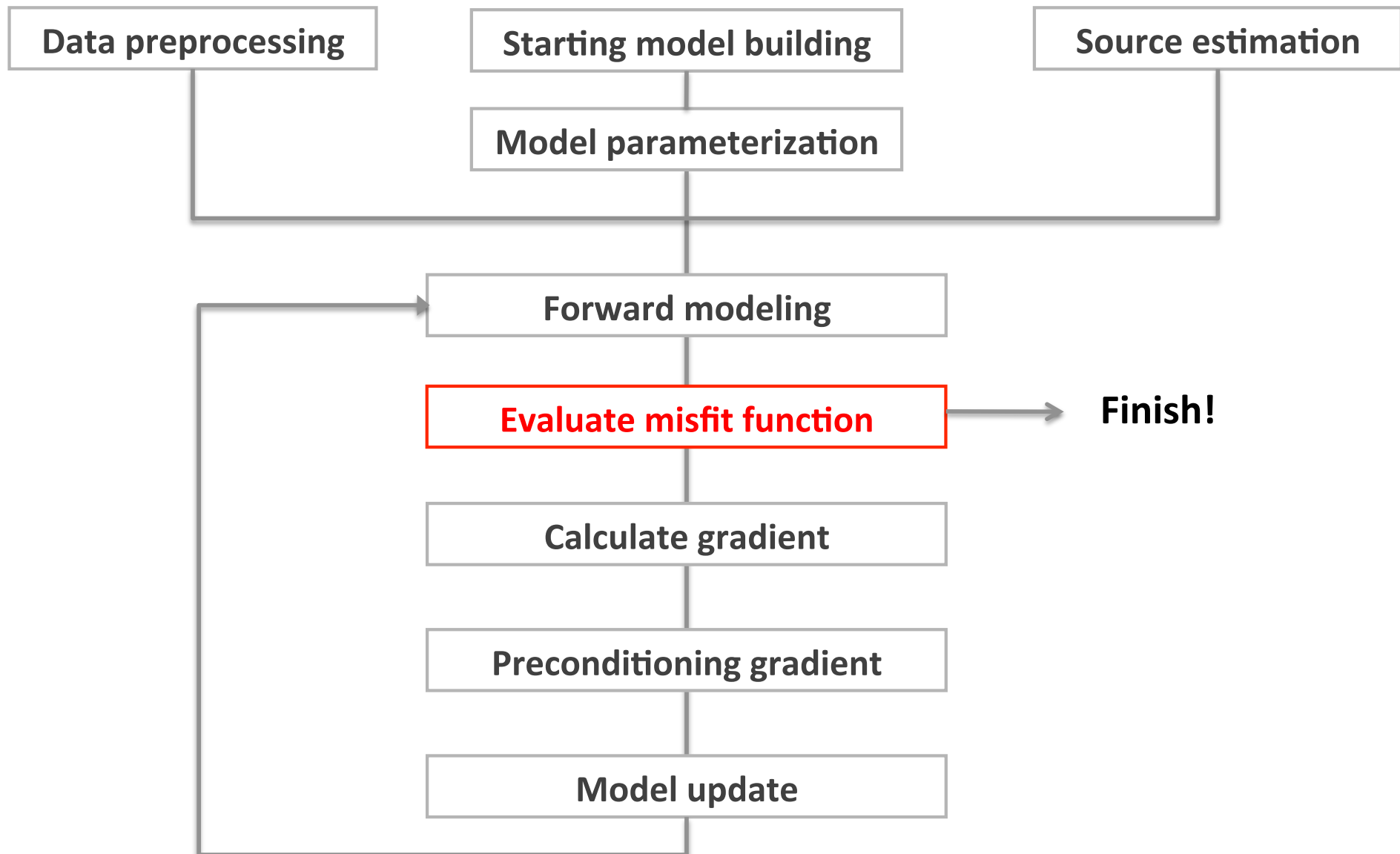
Workflow



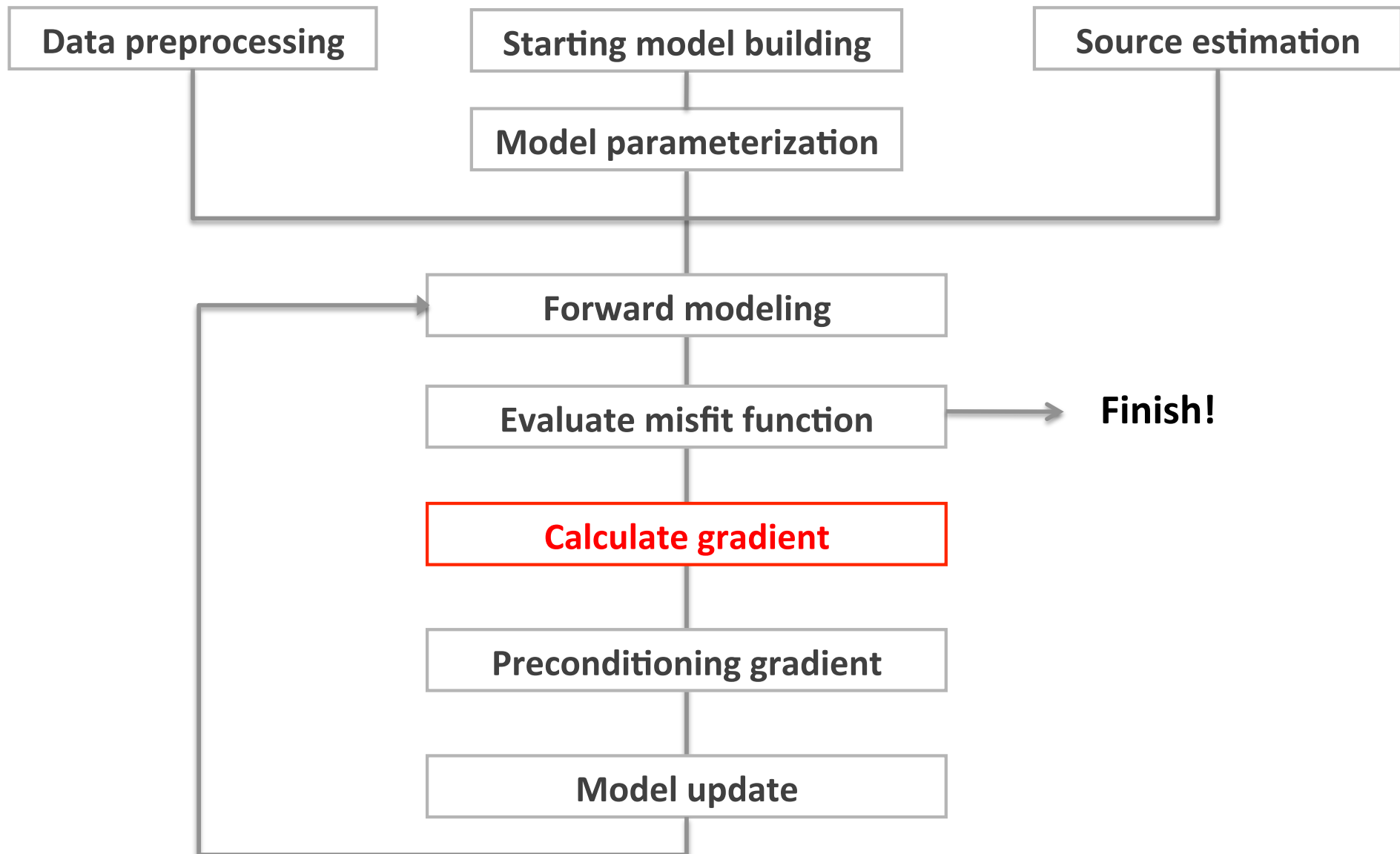
Workflow



Workflow

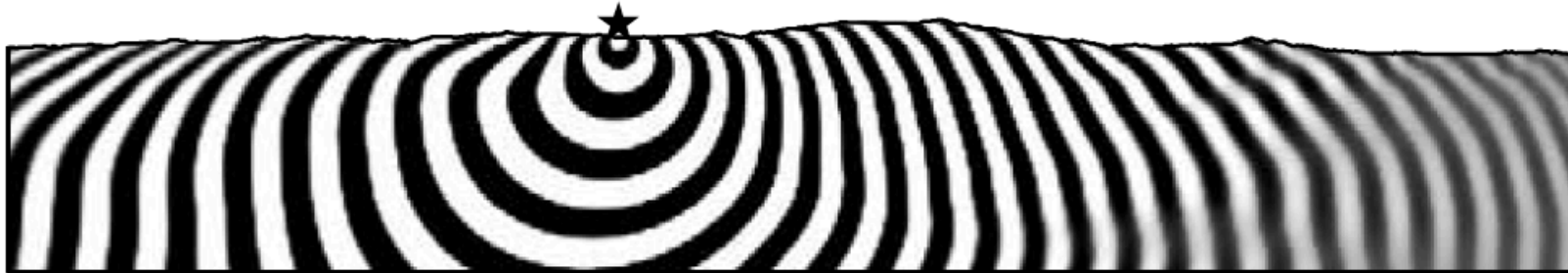


Workflow

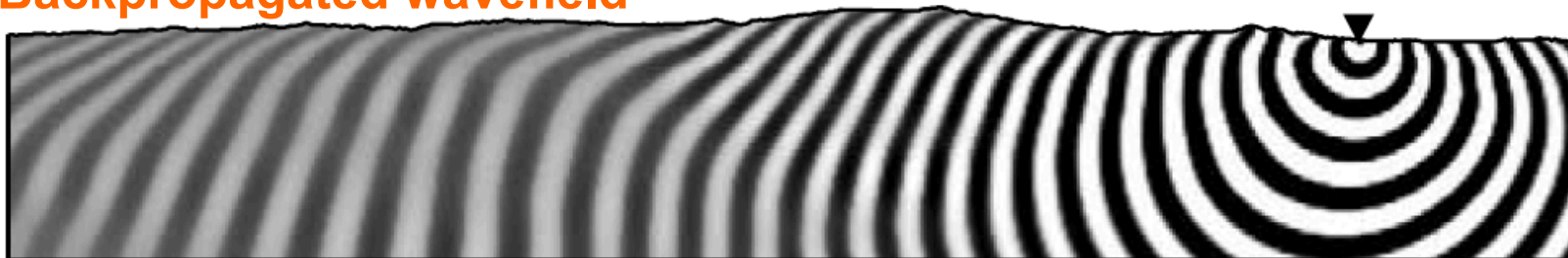


Gradient by adjoint method

Forward wavefield



Backpropagated wavefield

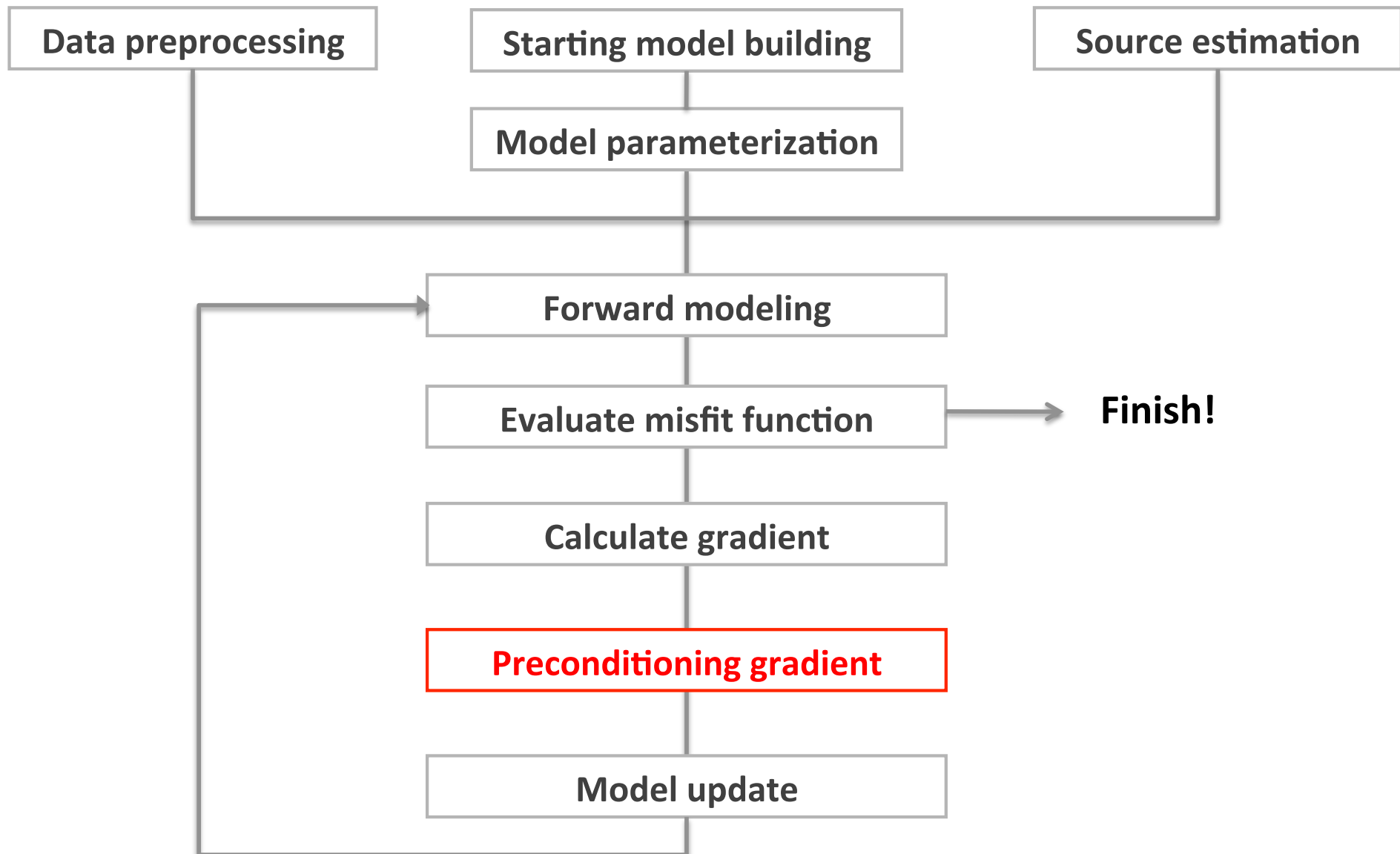


Gradient from a source-receiver pair

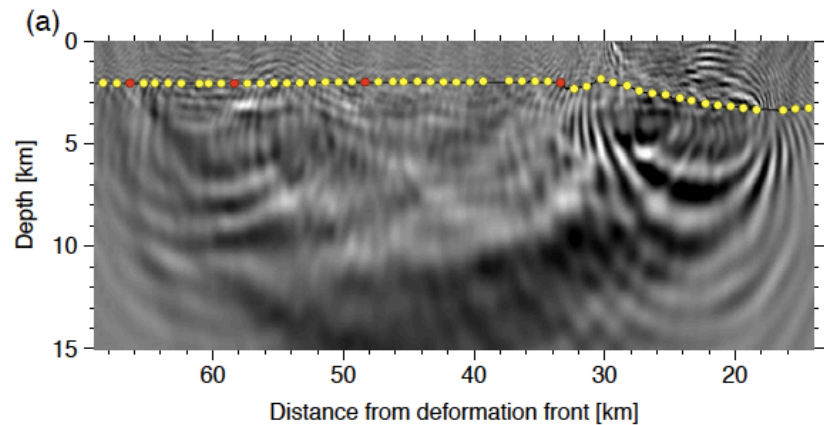


Bleibinhaus, F., Hole, J. A., Ryberg, T., & Fuis, G. S. (2007). *JGR*

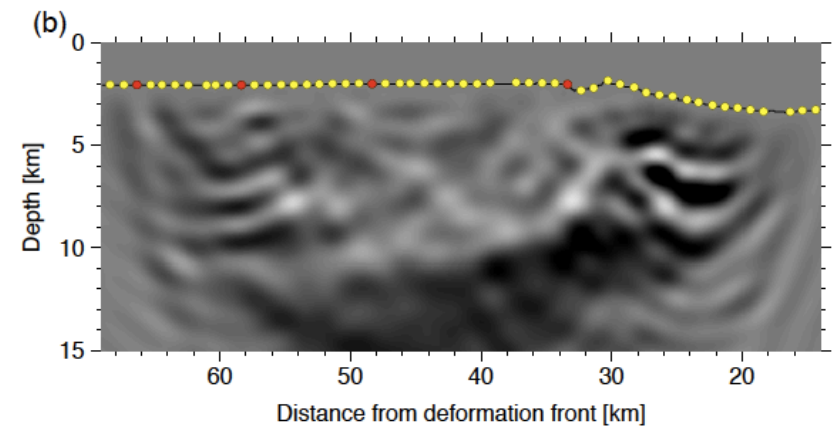
Workflow



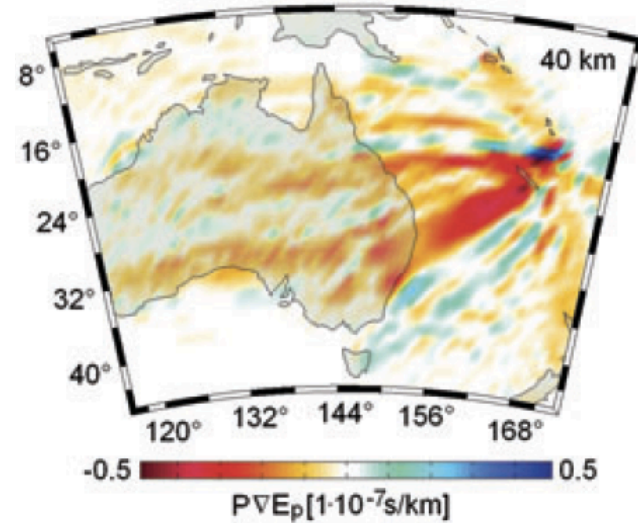
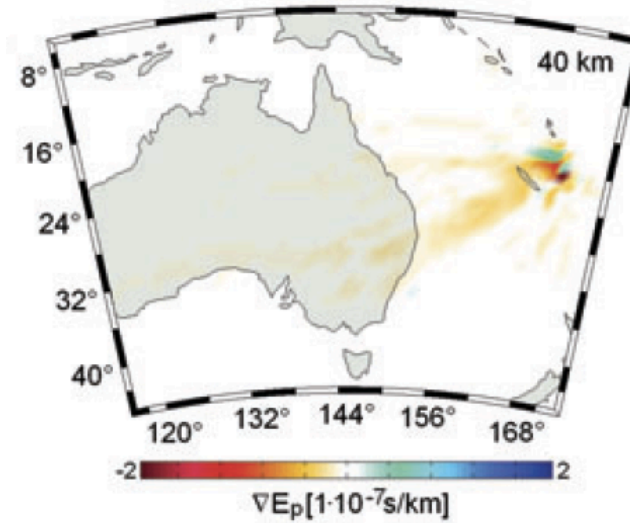
Raw gradient



Preconditioned gradient

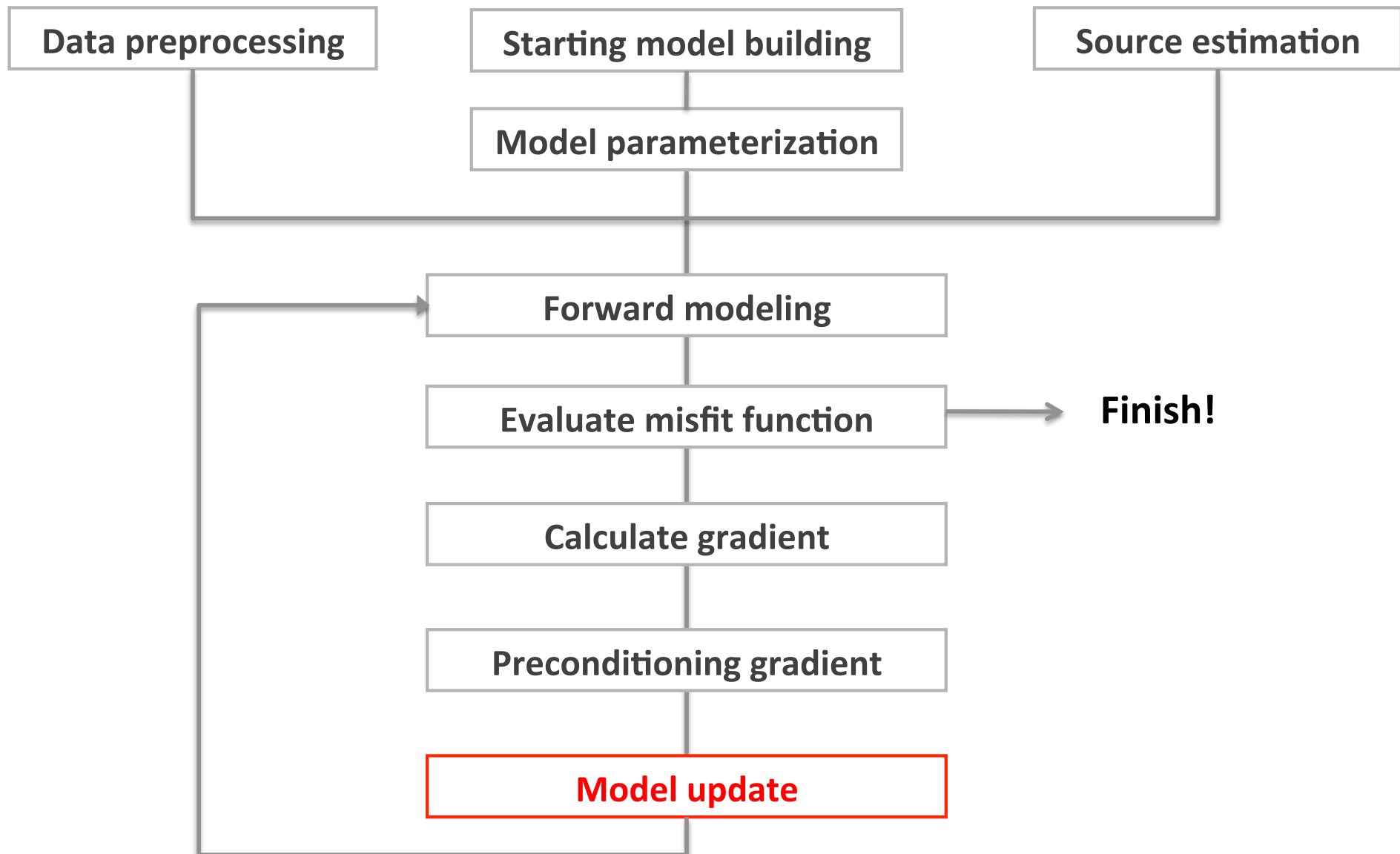


Kamei, R., Pratt, R. G., Tsuji, T., (2012), EPSL

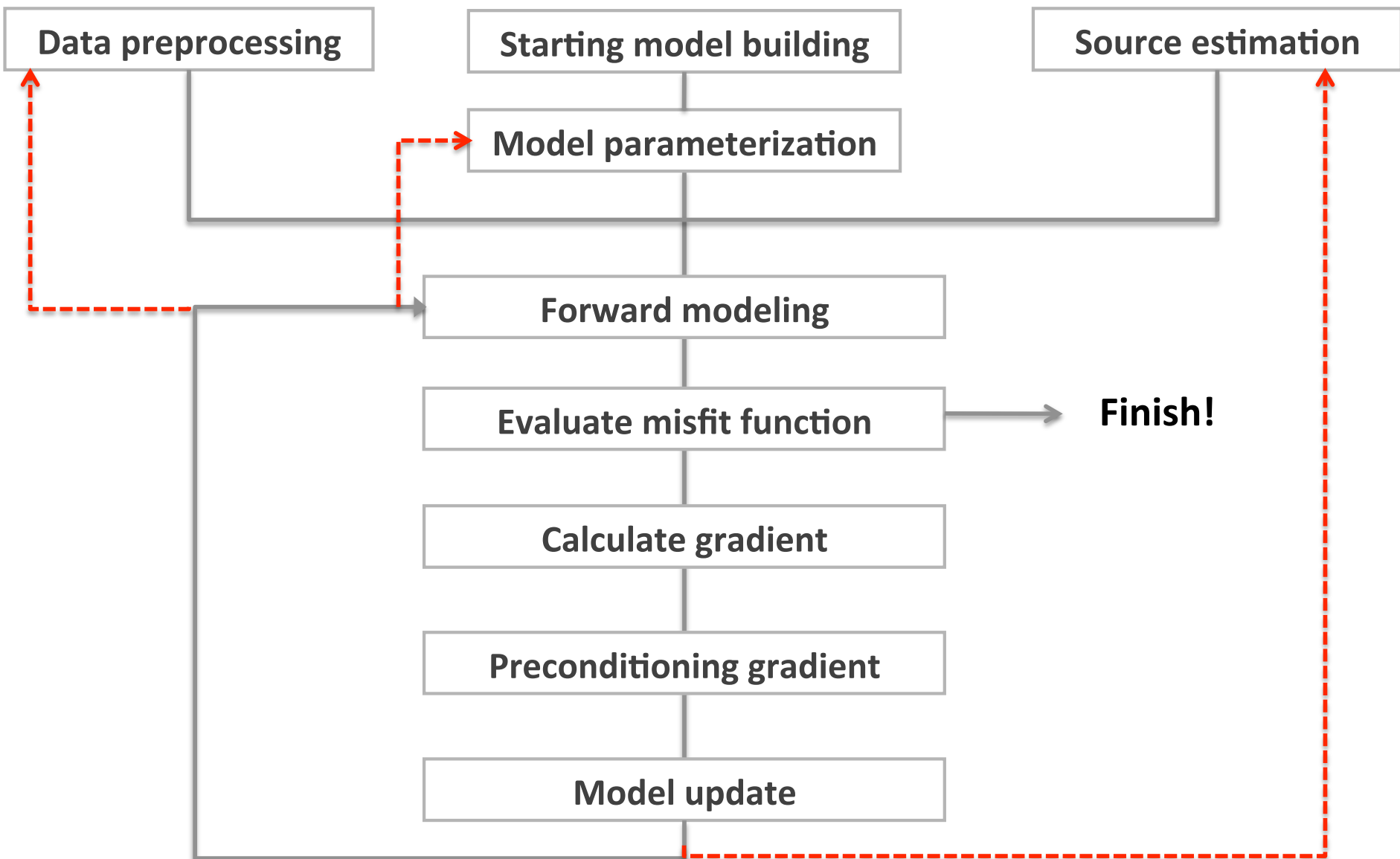


Fichtner, A., Kennett, B. L. N., Igel, H., & Bunge, H.-P. (2009). GJI

Workflow



Workflow



Outline

- Waveform inversion
 - Problem statement
 - Workflow
- Examples: A tour through scales

Examples

1. Upper mantle structure (*Fichtner et al., 2009, GJI*)
2. Crustal structure (*Tape et al., 2010, GJI*)
3. Crustal structure (*Kamei et al., 2012, EPSL*)
4. 3D oil/gas exploration (*Sirgue et al., 2010, Fast Break*)
5. Cross-well gas hydrate exploration (*Pratt et al., 2004, GSC Bulletin*)

Examples

Passive sources

1. Upper mantle structure (*Fichtner et al., 2009, GJI*)
2. Crustal structure (*Tape et al., 2010, GJI*)
3. Crustal structure (*Kamei et al., 2012, EPSL*)
4. 3D oil/gas exploration (*Sirgue et al., 2010, Fast Break*)
5. Cross-well gas hydrate exploration (*Pratt et al., 2004, GSC Bulletin*)

Examples

Active sources

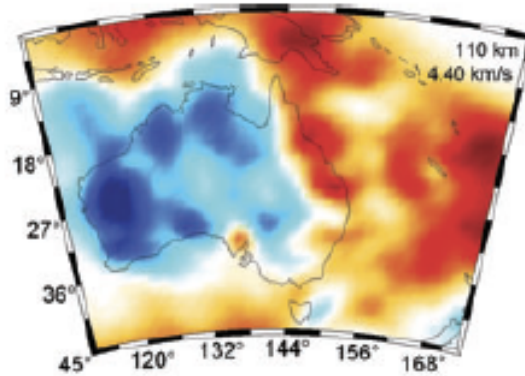
1. Upper mantle structure (*Fichtner et al., 2009, GJI*)
2. Crustal structure (*Tape et al., 2010, GJI*)
3. Crustal structure (*Kamei et al., 2012, EPSL*)
4. 3D oil/gas exploration (*Sirgue et al., 2010, Fast Break*)
5. Cross-well gas hydrate exploration (*Pratt et al., 2004, GSC Bulletin*)

Examples

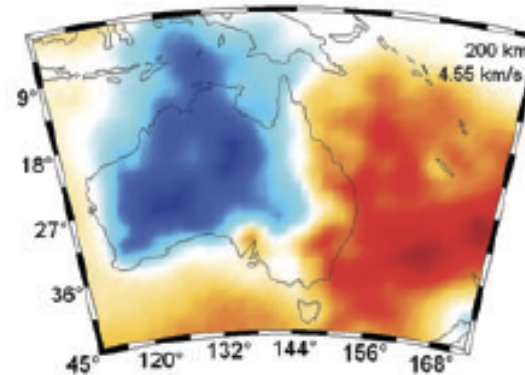
1. Upper mantle structure (*Fichtner et al., 2009, GJI*)
2. Crustal structure (*Tape et al., 2010, GJI*)
3. Crustal structure (*Kamei et al., 2012, EPSL*)
4. 3D oil/gas exploration (*Sirgue et al., 2010, Fast Break*)
5. Cross-well gas hydrate exploration (*Pratt et al., 2004, GSC Bulletin*)

Ex 1: Upper mantle structure beneath Australia

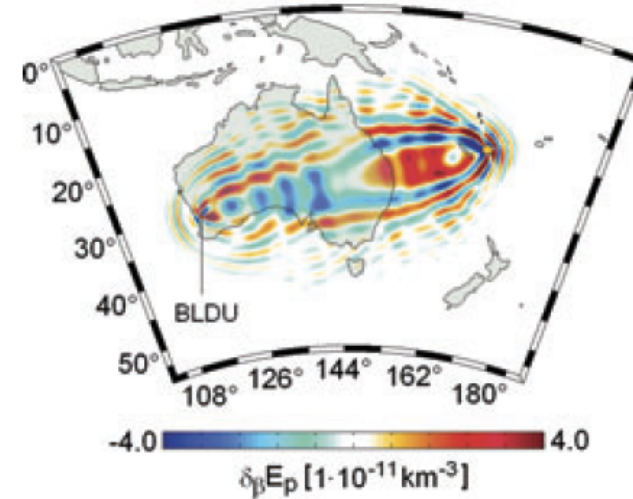
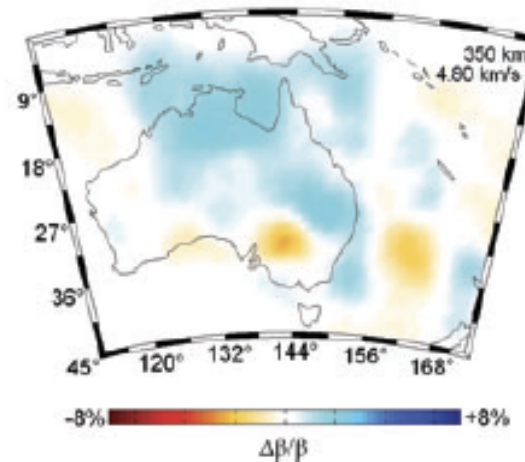
110 km



200 km



350 km



Target:
Upper-mantle structure

Frequency: 1/250 – 1/30 Hz

Wavelength: 135 – 1125 km

Distance: < 800 km

Scale: **5 – 37 λ**

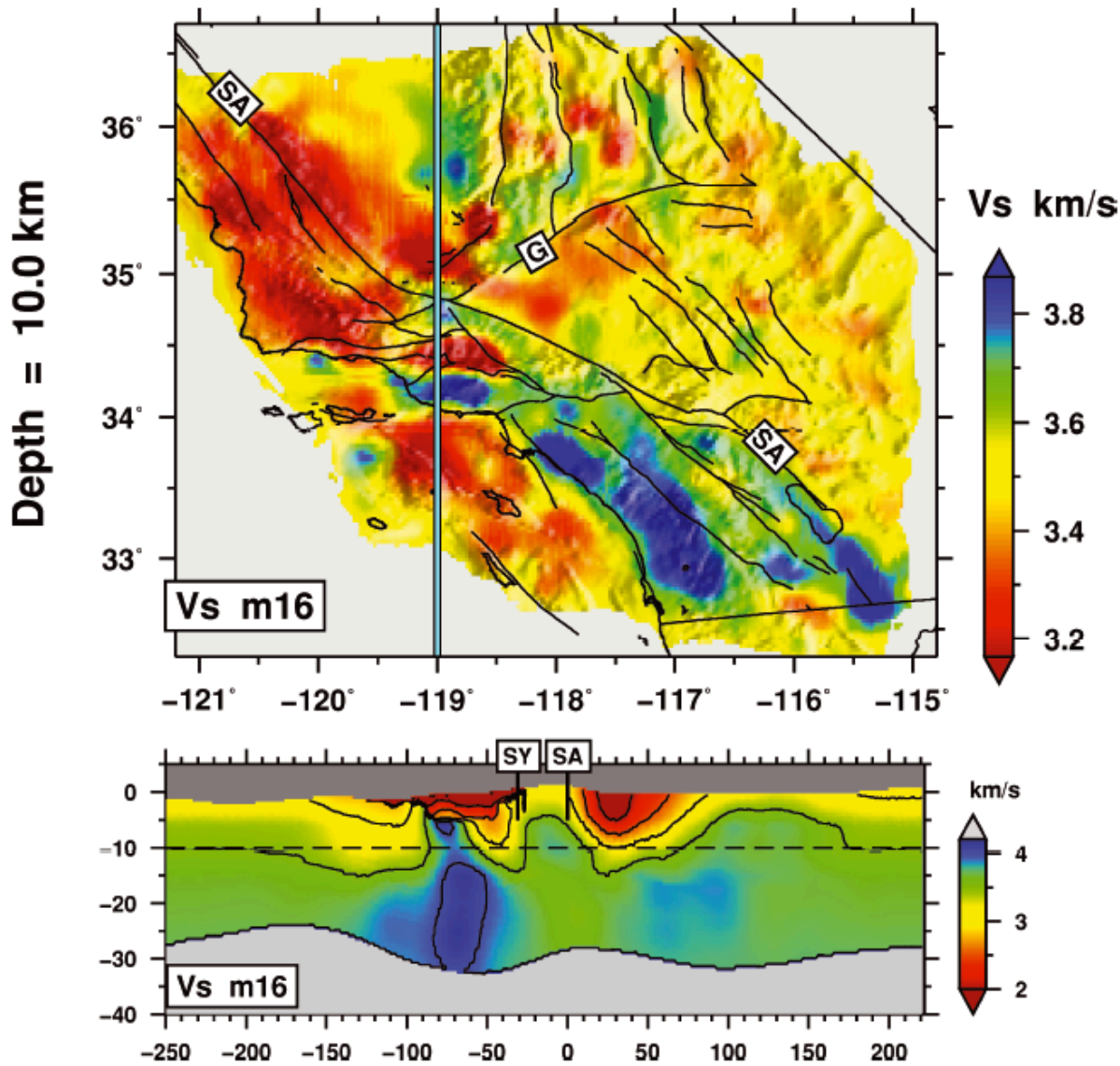
event: 57

traces: ~1000

iteration: 10

3D viscoelastic

Ex 2: Crustal imaging: Southern California



Tape, C., Liu, Q., Maggi, A., & Tromp, J. (2010). GJI

Target:
Basin
Composition across Fault

Frequency: 1/30 – 1/2 Hz

Wavelength: 8 – 120 km

Offset: < 800 km

Scale: **7–35 λ**

event: 143

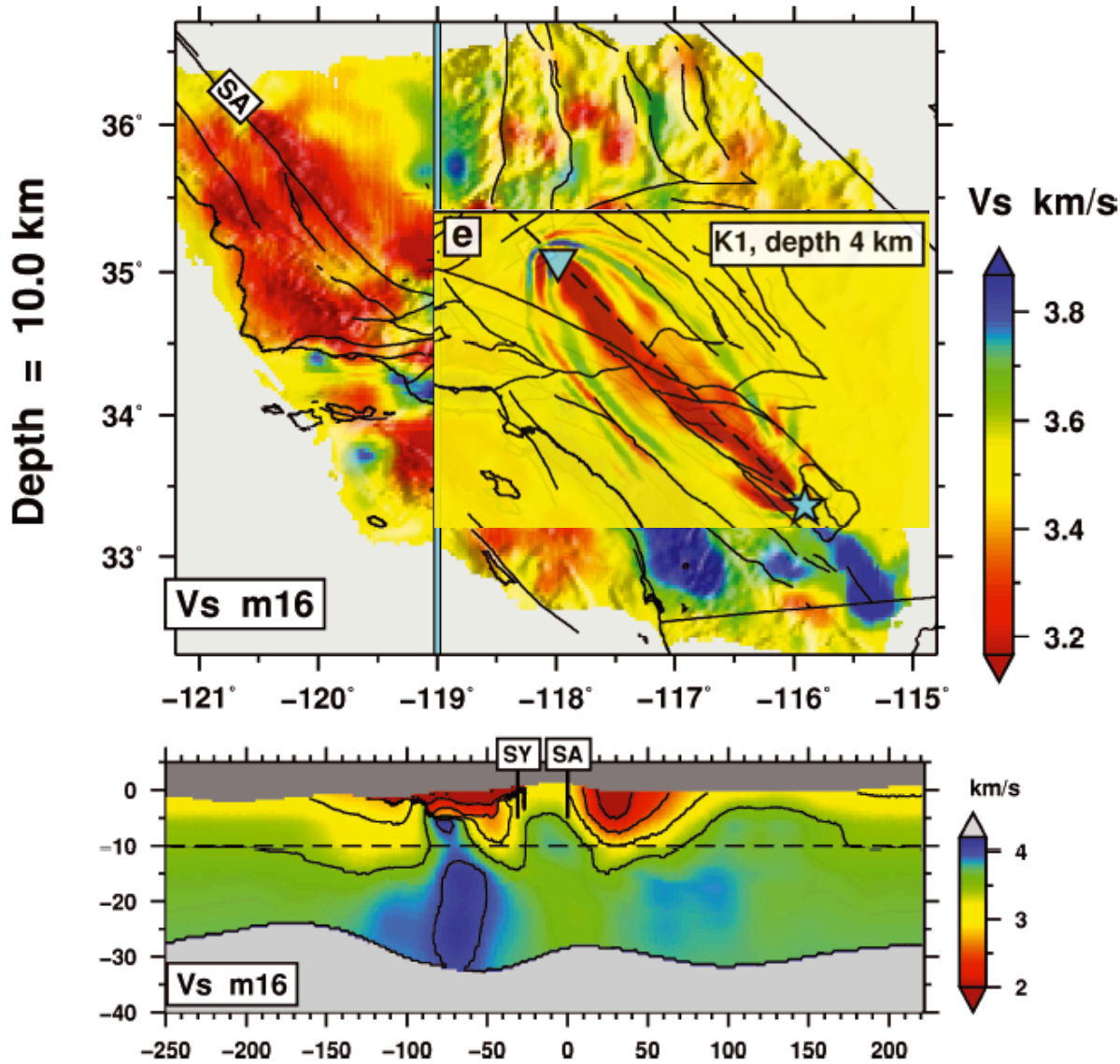
receiver: 203

traces: 52,000

iteration: 16

3D viscoelastic

Ex 2: Crustal imaging: Southern California



Tape, C., Liu, Q., Maggi, A., & Tromp, J. (2010). GJI

Target:
Basin
Composition across Fault

Frequency: 1/30 – 1/2 Hz

Wavelength: 8 – 120 km

Offset: < 800 km

Scale: **7–35 λ**

event: 143

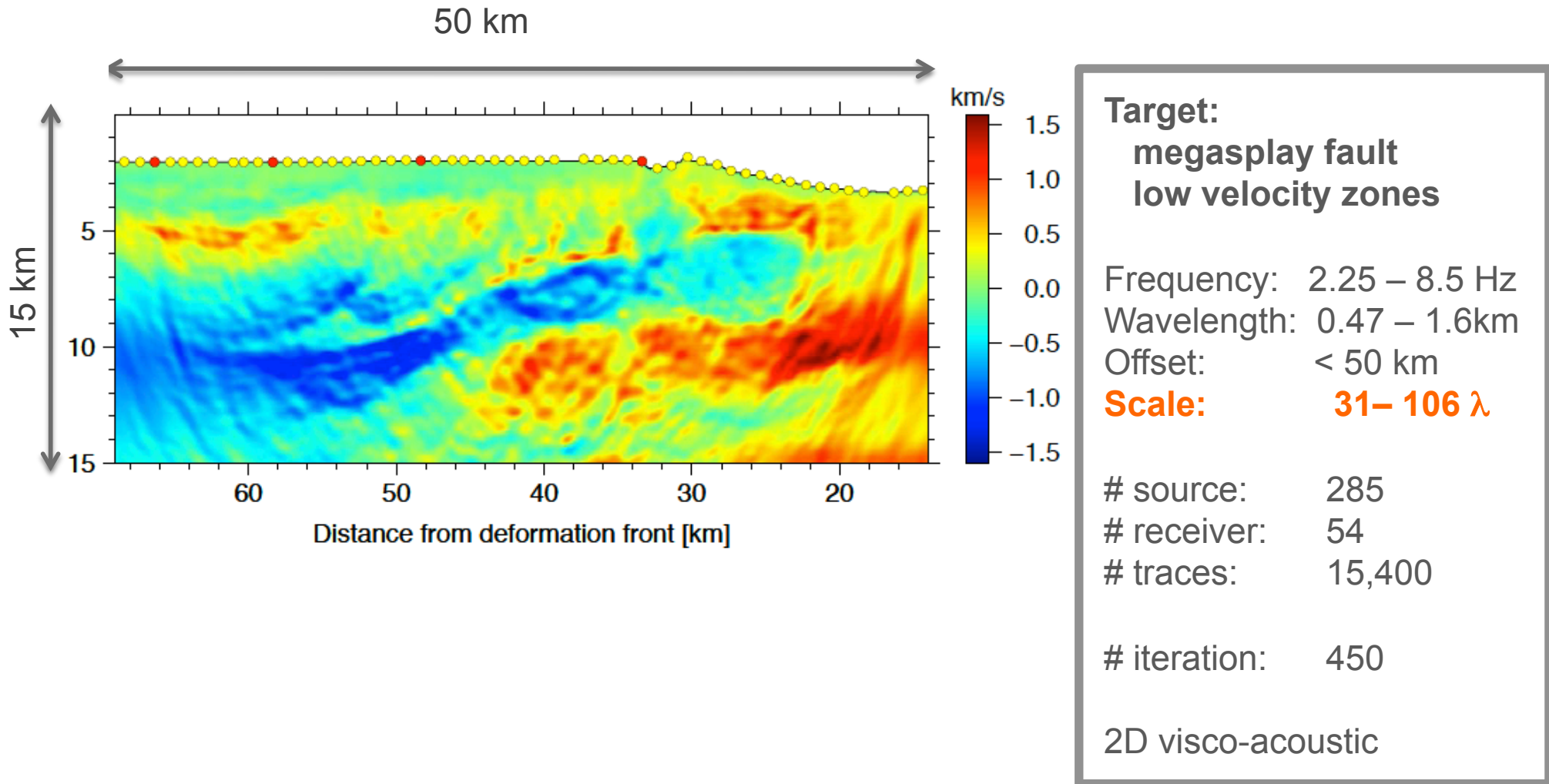
receiver: 203

traces: 52,000

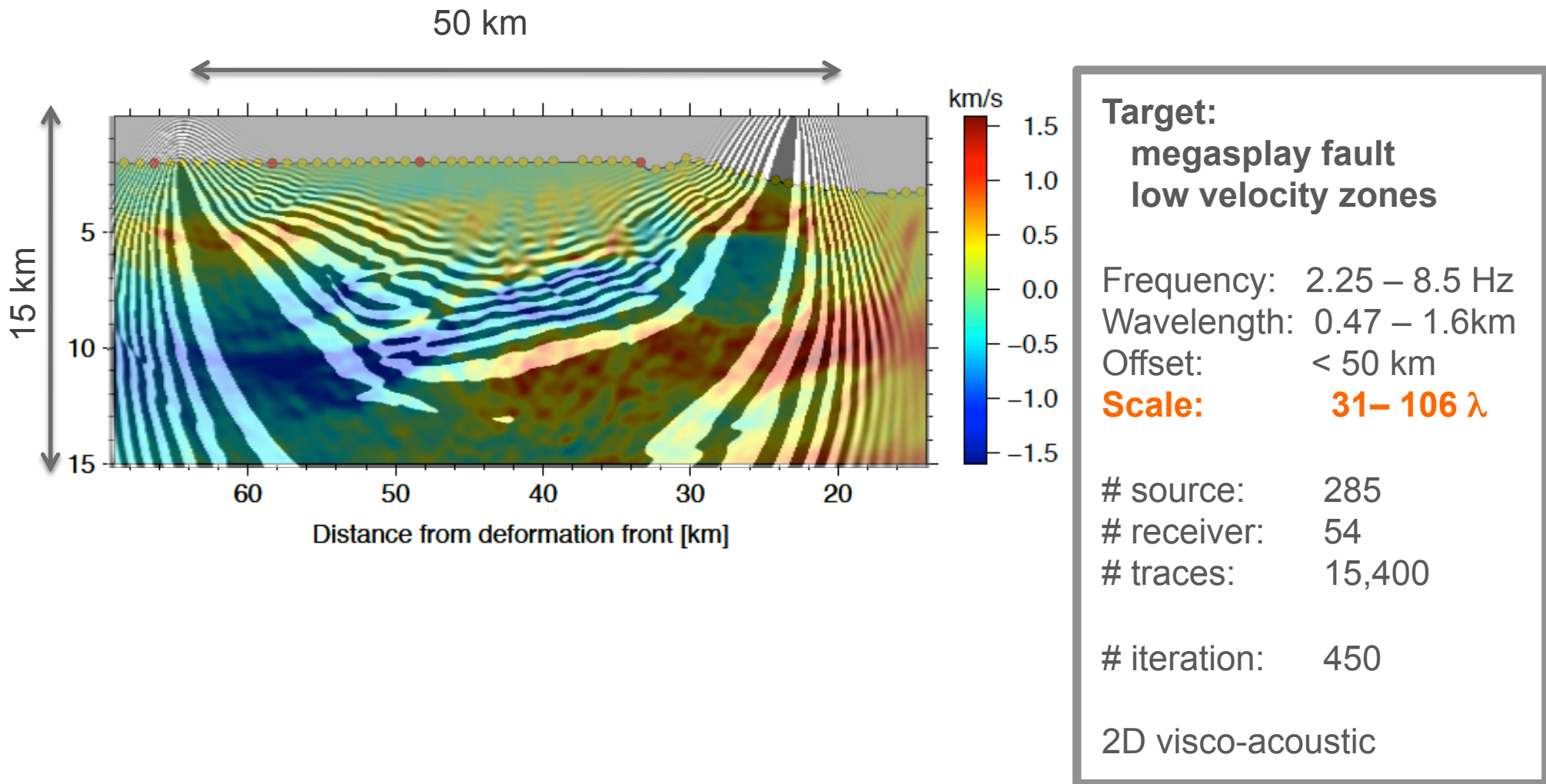
iteration: 16

3D viscoelastic

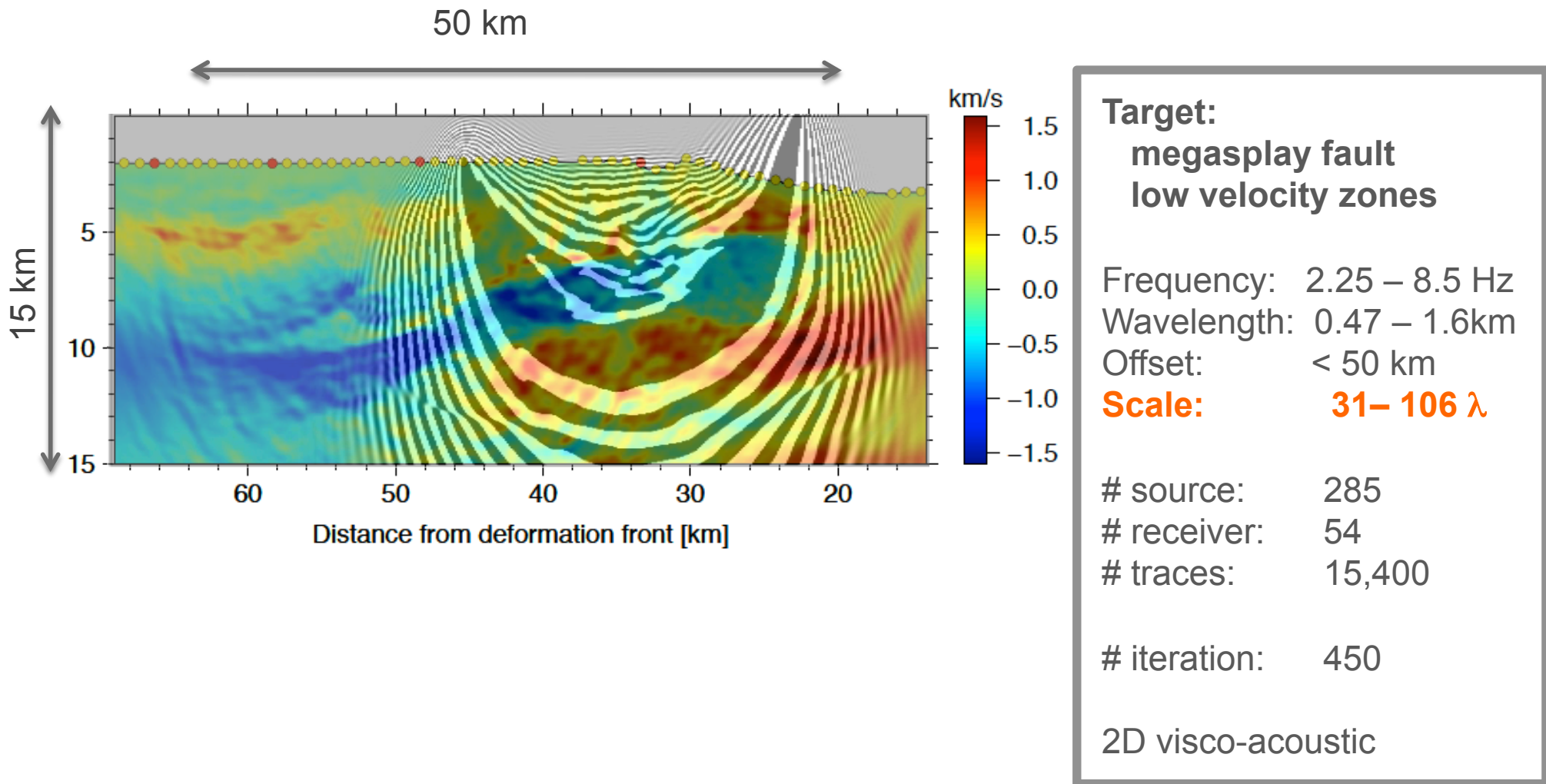
Ex 3: Crustal imaging in Nankai subduction zone



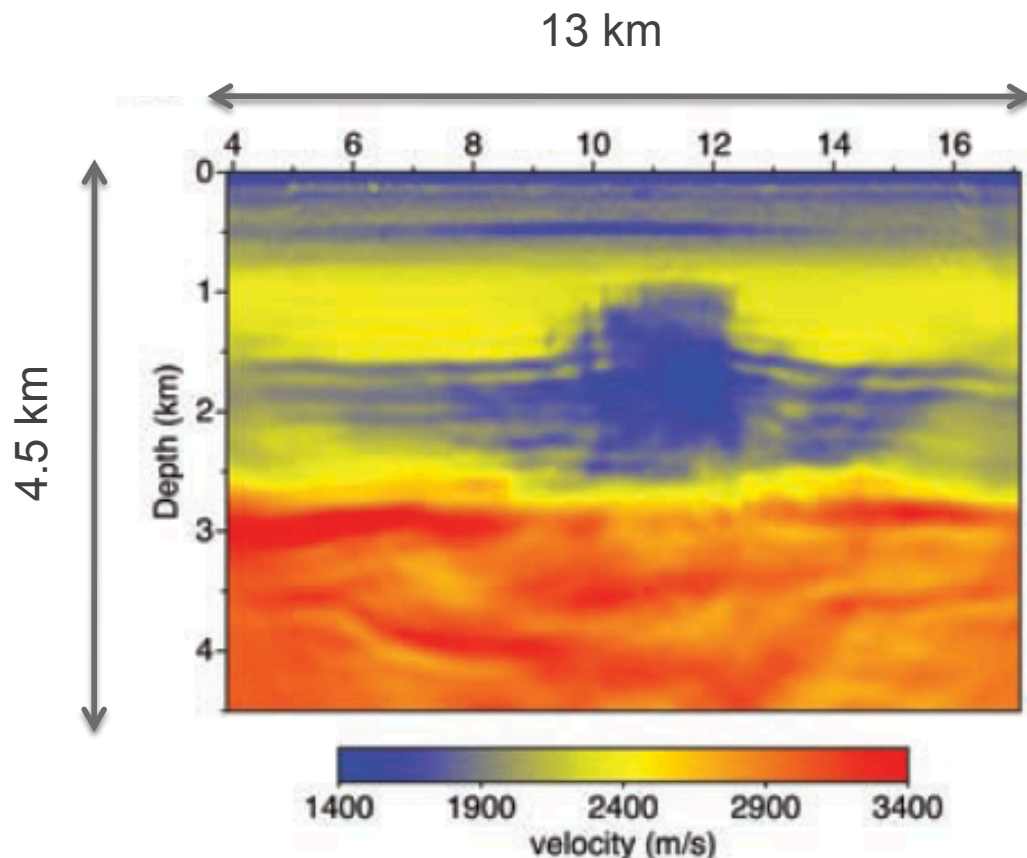
Ex 3: Crustal imaging in Nankai subduction zone



Ex 3: Crustal imaging in Nankai subduction zone



Ex 4: 3D oil exploration in Valhall, North sea



Target:

Oil reservoir
Gas chimney

Frequency: 3.5 - 7 Hz

Wavelength: 0.36 – 0.72 km

Offset: < 13 km

Scale: 18 – 36 λ

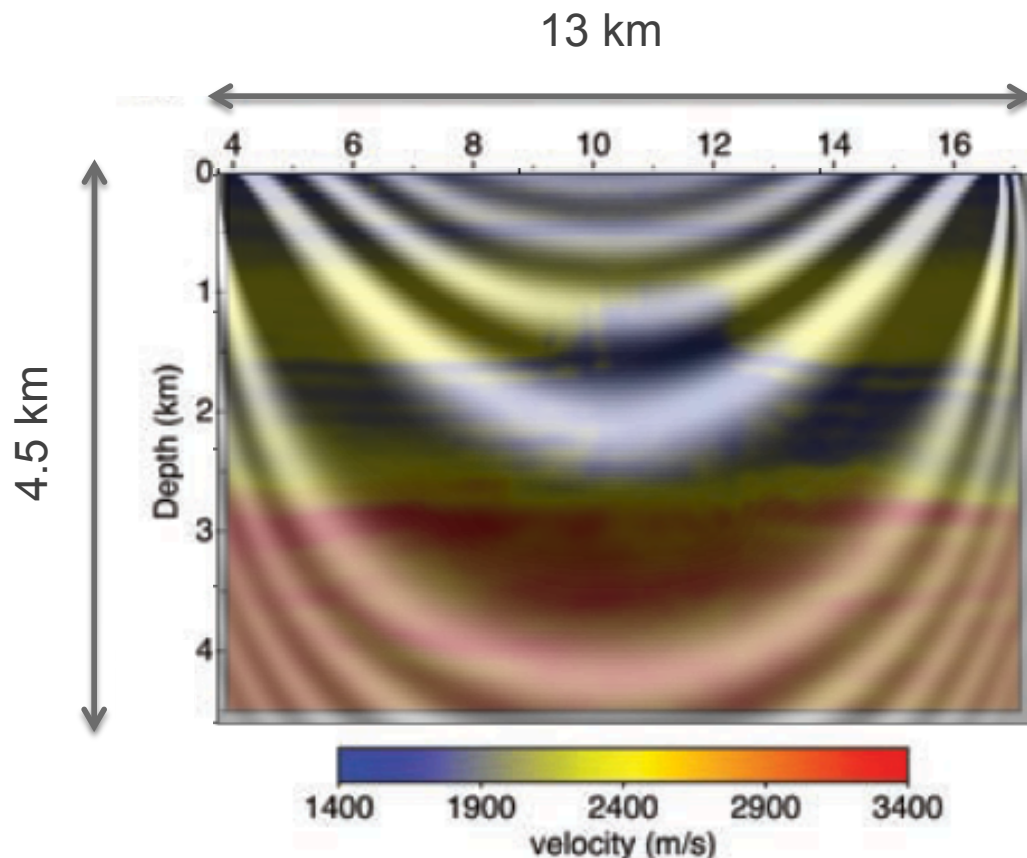
source: 50,000

receiver: 2,300

traces: 120,000,000

3D acoustic

Ex 4: 3D oil exploration in Valhall, North sea



Target:

Oil reservoir
Gas chimney

Frequency: 3.5 - 7 Hz

Wavelength: 0.36 – 0.72 km

Offset: < 13 km

Scale: 18 – 36 λ

source: 50,000

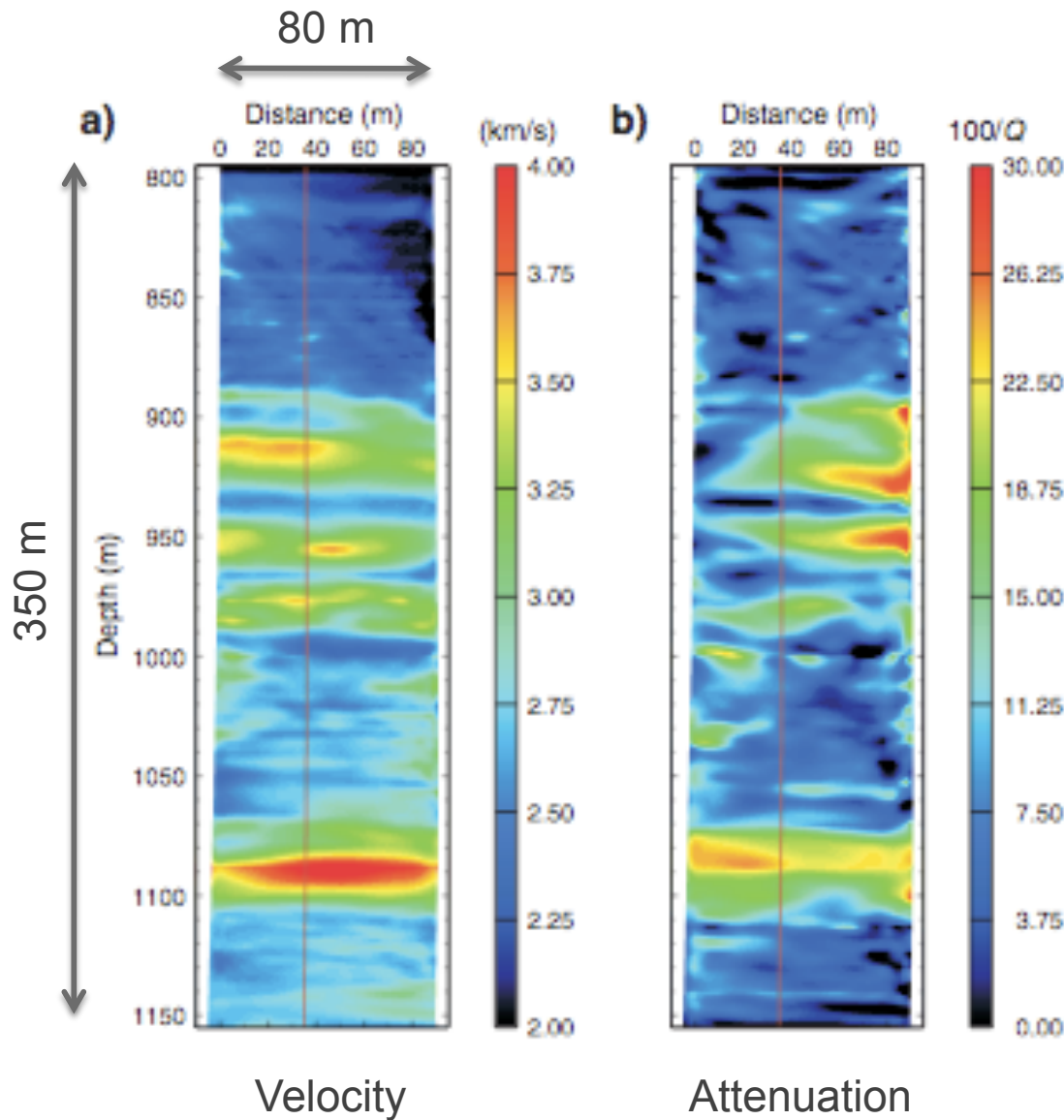
receiver: 2,300

traces: 120,000,000

3D acoustic

Sirgue, L., Barkved, O. I., Dellinger, J., Etgen, J., Albertin, U., & Kommedal, J. (2010). First Break
Etienne, V., Hu G., Operto, S. & Virieux, J. (2012) EGU

Ex 5: Gas hydrate production in Arctic Canada



Target:
Hydrate zone
(high velocity, high Q^{-1})

Frequency: 100 -1000 Hz

Wavelength: 3 – 30 m

Offset: < 128 m

Scale: 4 – 42 λ

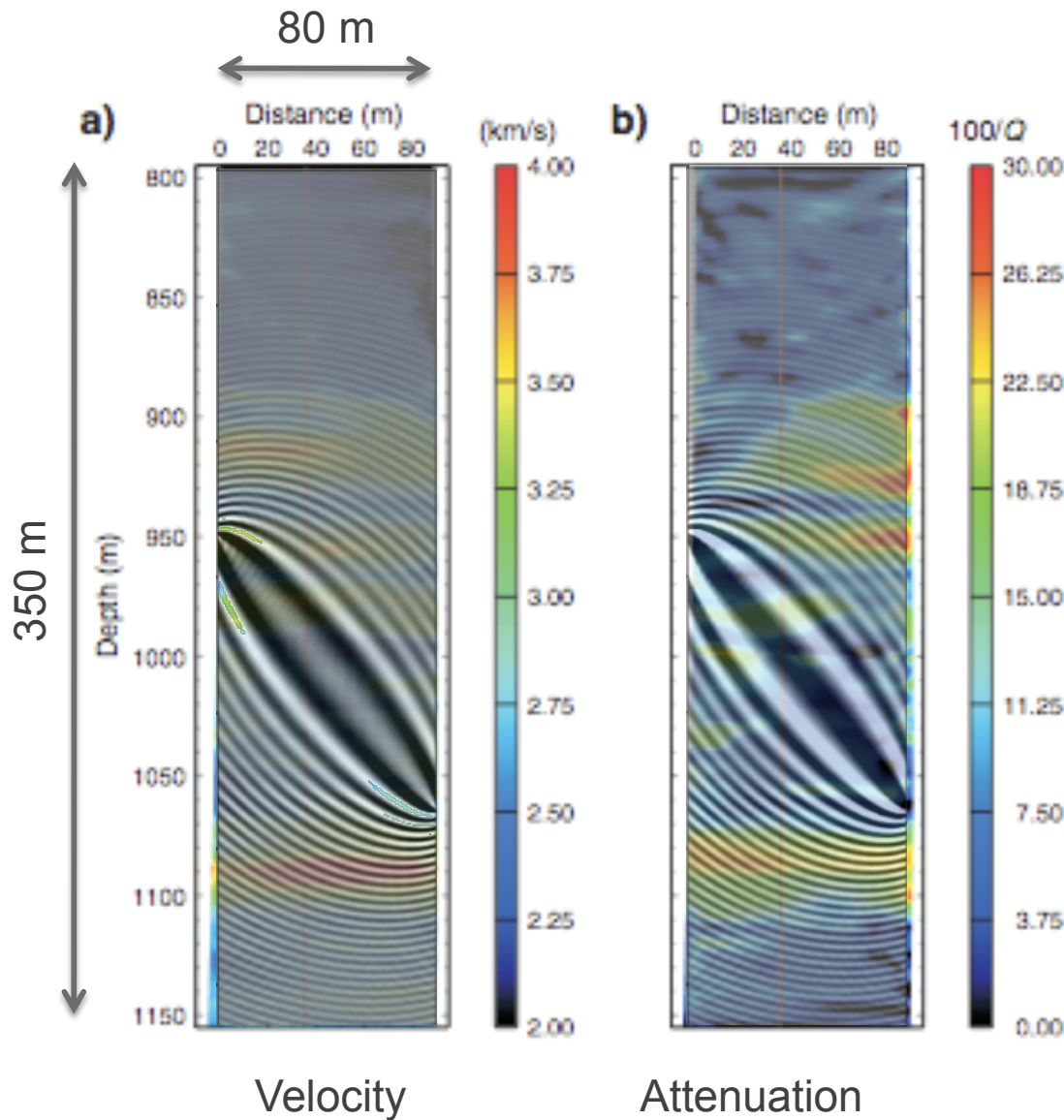
source: 454

receiver: 480

traces: 150,000

2D Visco-acoustic
Elliptic anisotropy

Ex 5: Gas hydrate production in Arctic Canada



Target:
Hydrate zone
(high velocity, high Q^{-1})

Frequency: 100 -1000 Hz

Wavelength: 3 – 30 m

Offset: < 128 m

Scale: 4 – 42 λ

source: 454

receiver: 480

traces: 150,000

2D Visco-acoustic
Elliptic anisotropy

	Active source	Passive source
Frequency	$1\text{-}10^3$ Hz	$10^{-3} \text{--} 10^{-1}$ Hz
Model size	crosswell – crustal 1-100s of wavelengths	local, regional, global 1-100s of wavelengths
Iteration	2D: $O(100)$, 3D: $O(10)$	$O(10)$
Survey geometry	regular, dense	irregular, sparse
Data	Pressure	3 components (Shear)
Data volume	2D: $O(1000)\text{-}O(100\,000)$ 3D: $O(10^6)$	$O(1000)\text{-}O(10,000)$
Forward modelling	Acoustic, FDM	Elastic, SEM, FDM
Starting model	Previous work Traveltime/Reflection tomography	Previous work CRUST2.0
Inversion domain	Frequency domain Time domain	Time-frequency domain Time domain
Misfit function	L2 (L1) data misfit L2 logarithmic misfit L2 phase misfit	L2 phase misfit L2 cross-correlation misfit

	Active source	Passive source
Challenges		Non-linearity Non-uniqueness Computational cost (3D) Model appraisal Resolution analysis Multi parameter
	data volume starting model topography	moment tensor irregular coverage crust, CMB

**Thank you very much
for your attention!**

Multiscale approach

Large scale features

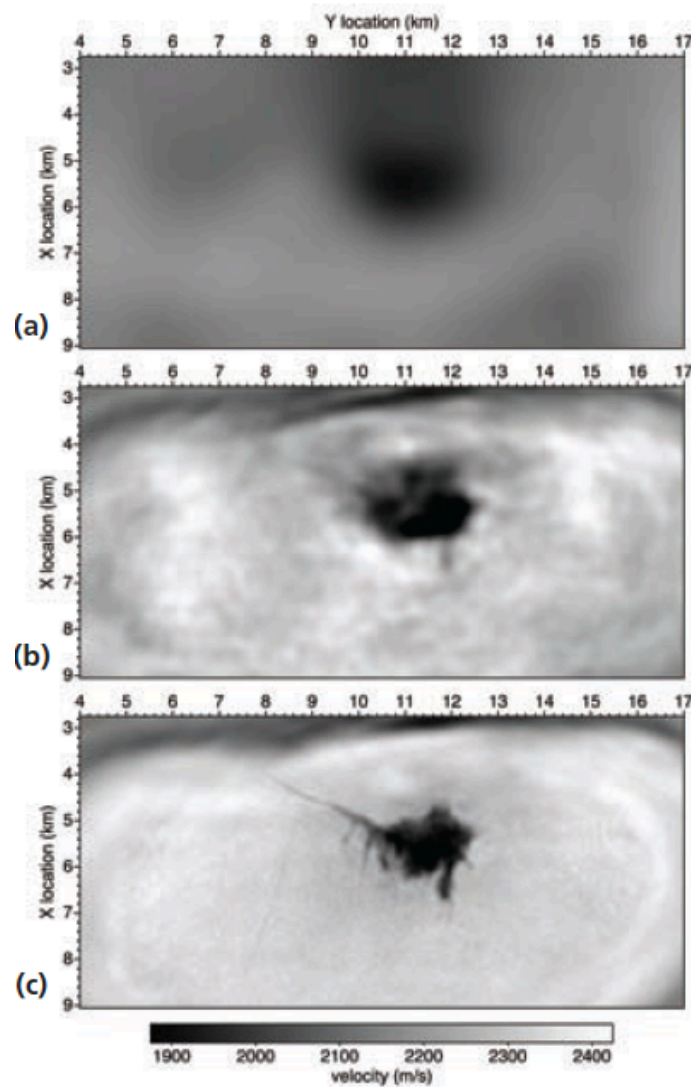
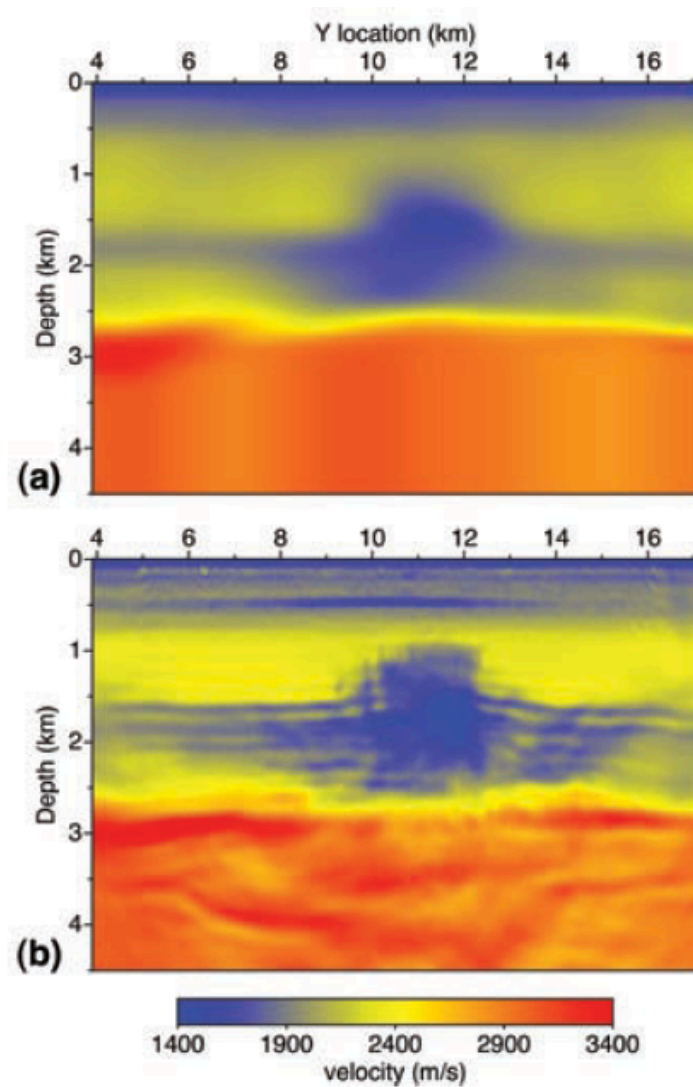
Small scale features



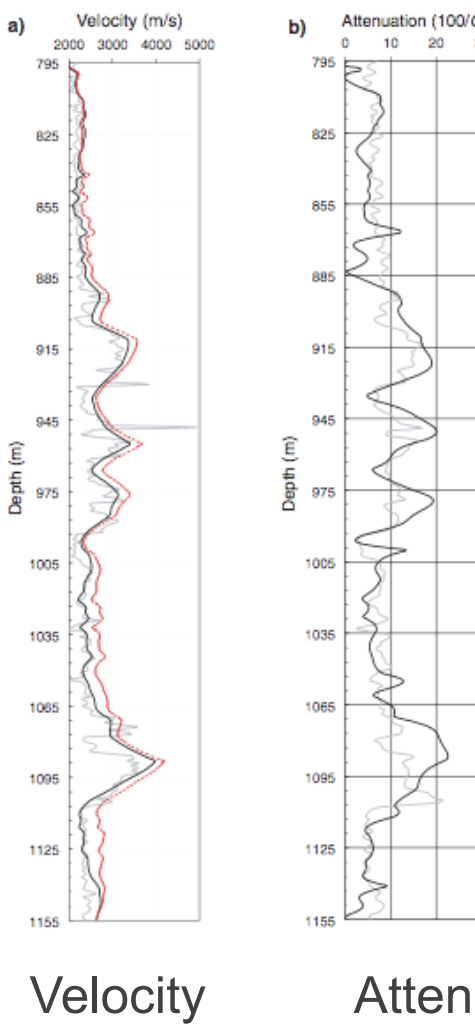
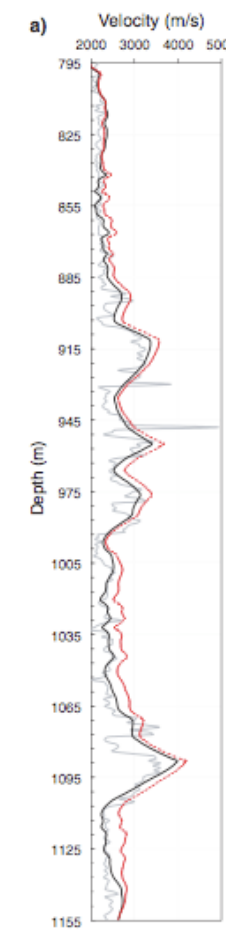
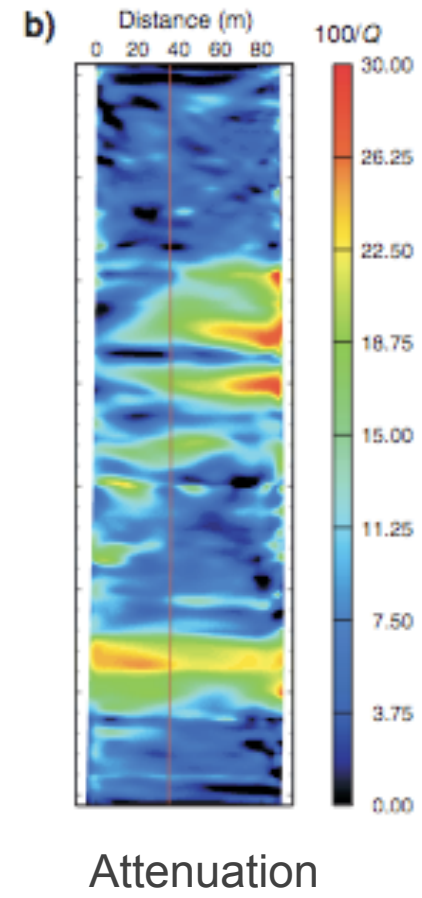
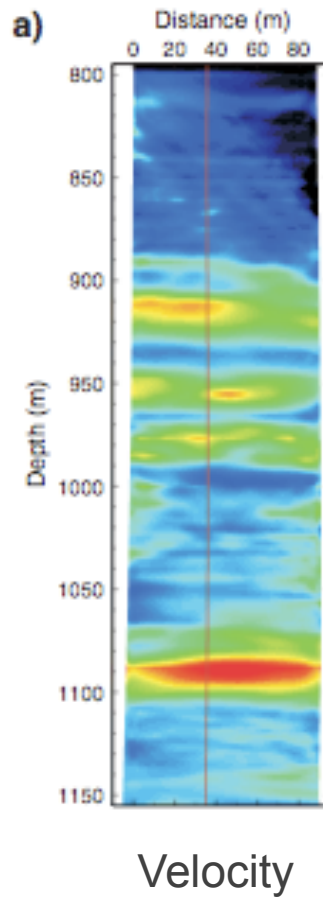
Low frequency component
Early arrivals

High frequency component
Later scattered arrivals

Ex 3: 3D Gas exploration in Valhall, North sea

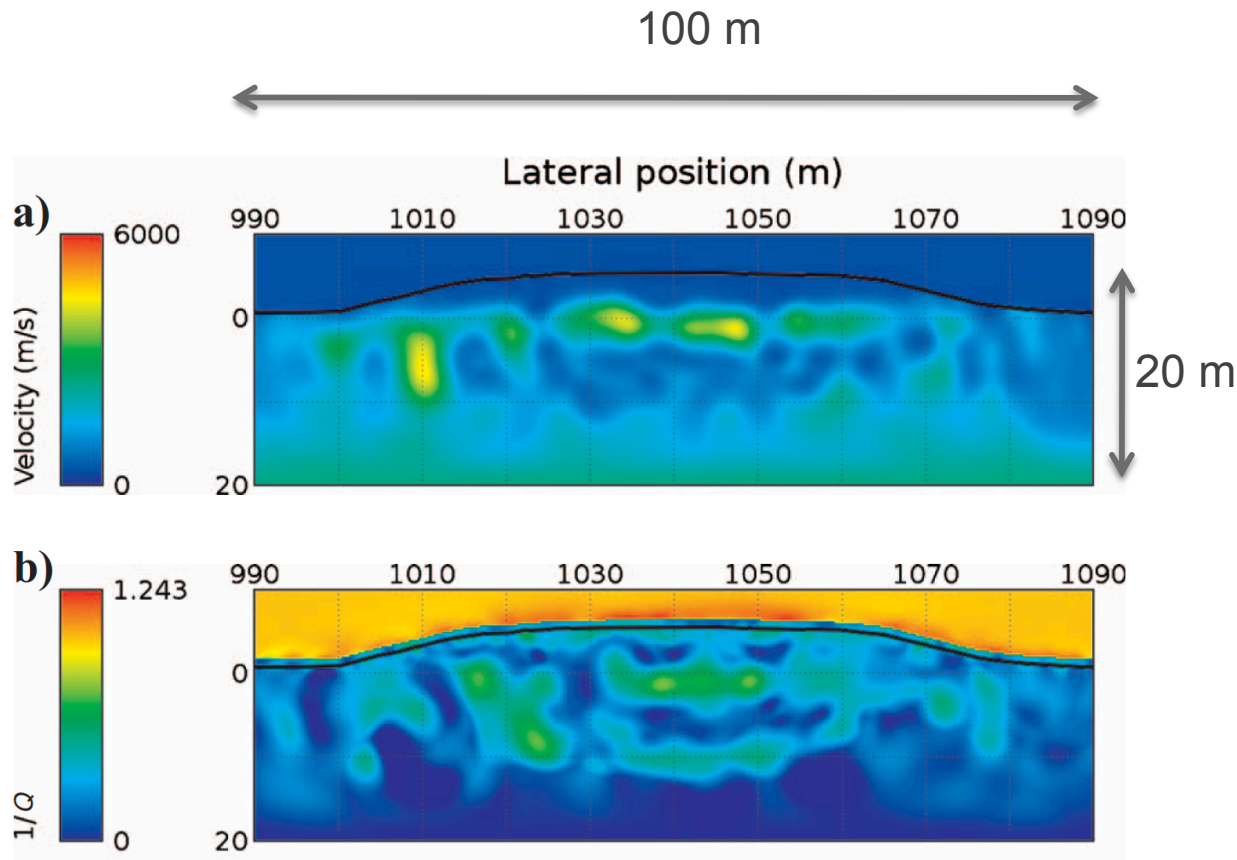


Gas hydrate production monitoring in Arctic Canada



Pratt et al. (2004)

Ex 5: Object detection of near surface



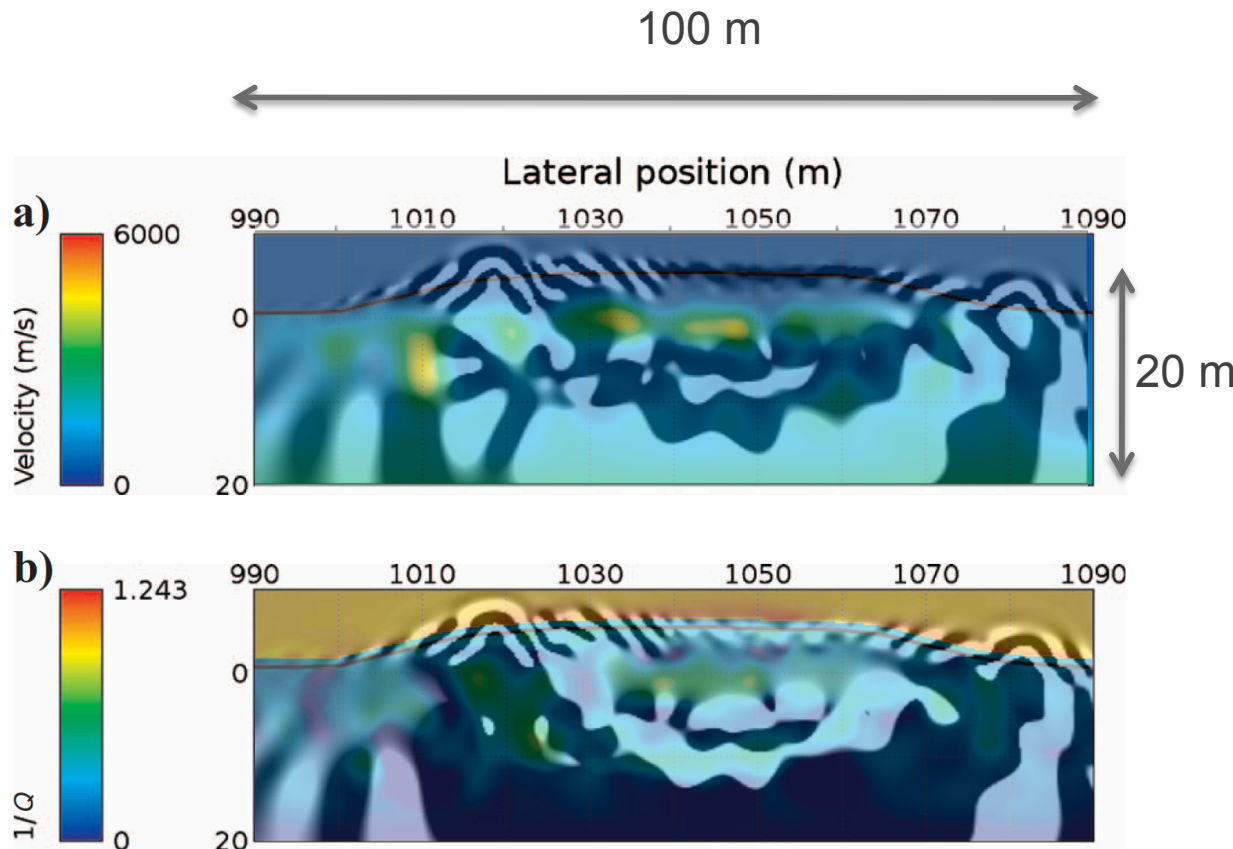
Frequency: 20 -150 Hz
Wavelength: 14 – 100 m
Offset: < 80 m
Scale: 0.8 – 5.7 λ

source: 70
receiver: 48
traces: 3360

Visco-acoustic

Smithyman et al. (2009)

Ex 5: Object detection of near surface



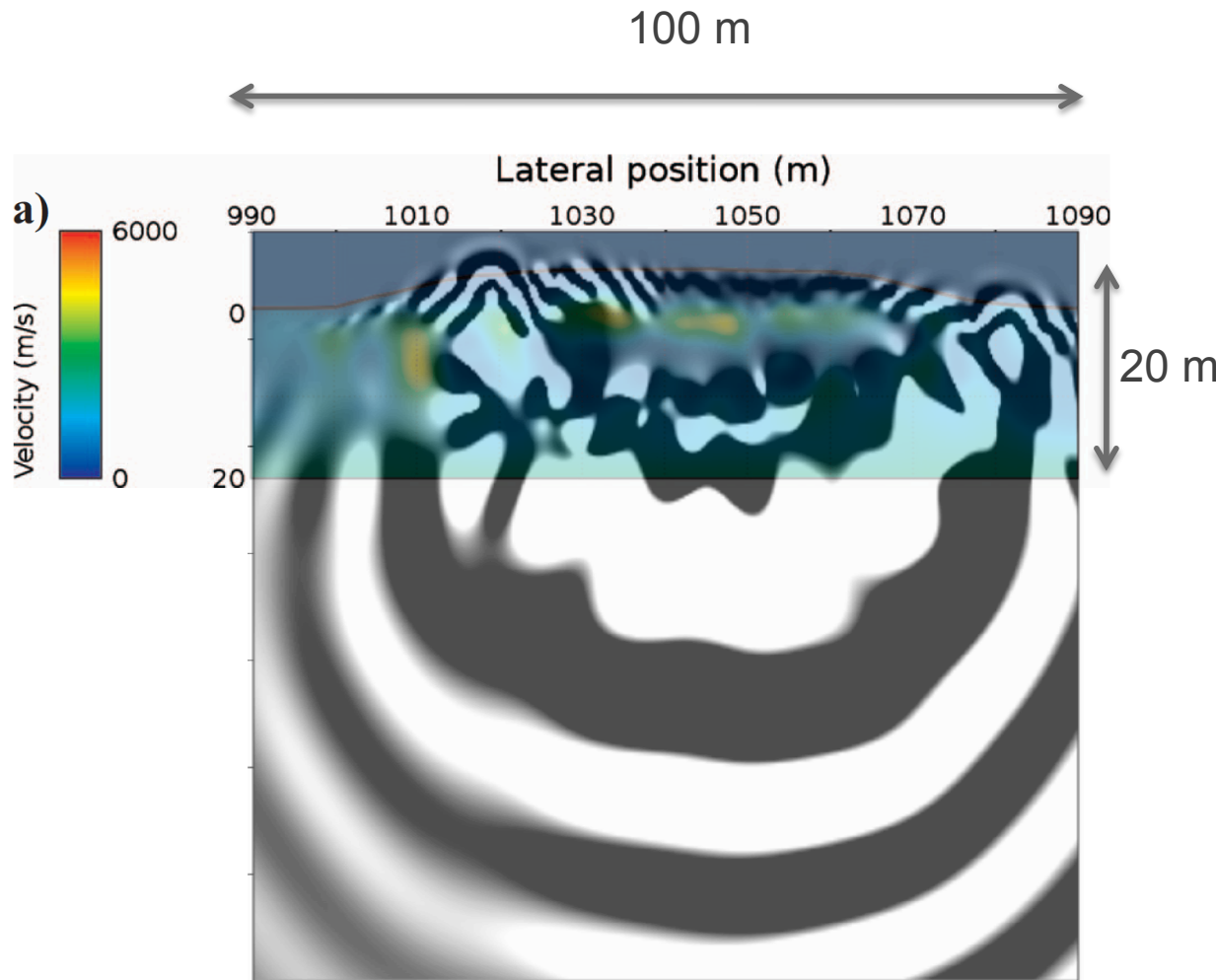
Frequency: 20 -150 Hz
Wavelength: 14 – 100 m
Offset: < 80 m
Scale: 0.8 – 5.7 λ

source: 70
receiver: 48
traces: 3360

Visco-acoustic

Smithyman et al. (2009) Geophysics

Ex 5: Object detection of near surface



Frequency:	20 -150 Hz
Wavelength:	14 – 100 m
Offset:	< 80 m
Scale:	0.8 – 5.7 λ
# source:	70
# receiver:	48
# traces:	3360
Visco-acoustic	

Smithyman et al. (2009) Geophysics